Master's thesis

NTNU
Norwegian University of Science and Technology
Faculty of Natural Sciences
Department of Chemistry

Natalie Storøy

Functionalized Graphene-based Ensembles for Carbon Capturing Membranes

Master's thesis in MLREAL

Supervisor: Solon Oikonomopoulos

June 2020

NTNU
Norwegian University of
Science and Technology

Natalie Storøy

Functionalized Graphene-based Ensembles for Carbon Capturing Membranes

Master's thesis in MLREAL
Supervisor: Solon Oikonomopoulos
June 2020

Norwegian University of Science and Technology
Faculty of Natural Sciences
Department of Chemistry

NTNU
Norwegian University of
Science and Technology

Preface

This master's thesis has been written in the spring of 2020 as a part of the Master of Natural Science with Teacher Education, at the Department of Chemistry, Norwegian University of Science and Technology. The thesis is relevant for my future work as a teacher as it addresses relevant topics from the curriculum in natural science and chemistry such as green chemistry and organic chemistry. In addition, having completed a master's program has given me a greater insight in how research is conducted, which can be valuable experience to share with future students. However, the circumstances have been quite surreal due to COVID19, with shutdown of the university and exclusion from the lab. This has affected the work with this master's thesis in the extent of changing it from an experimental thesis to a theoretical one.

I would like to thank my supervisor Solon Oikonomopoulos, for his guidance and feedback, and for his transmittable good mood and support through the whole process. I would also like to thank the co-students in the lab for valuable support and good company, for as long as it lasted.

I would like to thank Roger Aarvik and Torunn Melø for their technical support.

I would also like to thank my partner Kristian Moen Slotvik, my friends, and my family for being supportive and motivating me through this period writing this thesis. At last, I would like to thank Kristine Eide, Eirik Berg and Kristine Fjelldal Sunde for pleasant lunch breaks with a numerous of card games.

Abstract

In an effort to help deal with the impending climate crisis, an assortment of carbon capturing mixed matrix membranes enriched with functionalized graphene-based nanofillers were compared and evaluated based on their CO_2 permeability and CO_2/N_2 selectivity performances. The thesis attempts to present a comprehensive study on the most important literature results on this research area. Matrices such as polyimide (PI), poly(ether-block-amide) (PEBAx), sulfonated poly(ether ether ketone) (SPEEK), polysulfone (PSf), and ethyl cellulose (EC), in addition to an advanced copolymer (PEDM) were analysed after being "doped" with different graphene nanofillers. The functional units attached onto graphene involved imidazole groups, amino-groups, ionic liquids, metal organic frameworks (MOFs), zeolitic imidazole frameworks (ZIFs), ethylene oxide (EO) groups, sulfonated groups, and others.

Results showed that there was an increase in both permeability and selectivity along with an increase in the content filler. This trend was observed up to a certain optimized concentration, before a decrease for both properties occurred. Degradation of properties, was due to agglomeration of the graphene-based nanosheets, caused by interactions effects. The best membranes were obtained using PEBAx or SPEEK as polymers, under humidified conditions. Water was then participating in reactions with CO_2, increasing the diffusion. Incorporated nanofillers containing EO- or amino functionalized graphene were most promising due to EO's good affinity towards CO_2, increasing the solubility selectivity, and amine's reversible reactions with CO_2 when water was present, contributing to an enhanced reactivity selectivity. Inspirations for future work based on these results have also been suggested.

Sammendrag

I et forsøk på å håndtere den forestående klimakrisen ble et utvalg av karbonfangende sammensatte matriksmembraner, beriket med grafen-baserte nanofyllere, sammenlignet og evaluert på grunnlag av deres CO_2-permeabilitets- og CO_2/N_2 selektivitetspresentasjoner. Oppgaven forsøker å presentere en omfattende studie av de viktigste litteraturresultatene på dette forskningsområdet. Matriser som polyimid (PI), poly(eter block amid) (PEBAx), sulfonert poly(eter eter keton) (SPEEK), polysulfon (PSf), og etyl cellulose (EC), i tillegg til en avansert copolymer (PEDM) ble analysert etter å ha blitt «dopet» med ulike funksjonaliserte grafen-baserte nanofyllere. De funksjonaliserte enhetene involvert var imidazol grupper, amino-grupper, ioniske væsker, organiske metallrammeverk (MOFs), zeolitiske imidazolrammeverk (ZIFs), etylenoksid (EO) grupper, sulfonerte grupper med flere.

Resultatene viste at det var en økning i både permeabilitet og selektivitet sammen med en økning i fyllstoff. Denne trenden ble observert opp til en viss optimalisert konsentrasjon, før en nedgang inntraff for begge egenskapene. Nedgangen av egenskapene var forårsaket på grunn av agglomerering blant de grafen-baserte nanolagene, som var et resultat av interaksjonskrefter. De beste ytelsene ble oppnådd ved å benytte membraner av PEBAx eller SPEEK matriser som polymerere, under fuktige forhold. Vann deltok i reaksjoner med CO_2, som økte diffusjonen. Inkorporerte nanofyllere som inneholdt EO- og amino-grupper viste seg å være mest lovende, på grunn av EOs gode affinitet til CO_2 som økte løselighetsselektiviteten, og aminenes reversible reaksjoner med CO_2 når vann var til stede som medvirket til en forbedret reaktivitetsselektivitet. Forslag for fremtidig arbeid basert på disse resultatene har også blitt foreslått.

Table of content

Abbreviations

A-prGO – *Aminated partially reduced graphene oxide*

APTS – *3-aminopropyltriethoxysilane*

CCS – *Carbon capture and storage*

CNT – *Carbon nanotubes*

Cs – *Chitosan*

Cys – *Cysteine*

DA – *Dopamine*

DBU – *1,8-diazabicycloundec-7-ene*

EC – *Ethyl cellulose*

EG – *Epitaxial graphene*

EO – *Ethylene oxide*

FLG – *Few layered graphene*

GO – *Graphene oxide*

HEG – *Hydrogen exfoliated graphene*

HPEI – *Hyperbranched poly-ethyleneimine*

IL – *Ionic liquid*

Im – *Imidazole*

IPCC – *Intergovernmental Panel on Climate Change*

MMM – *Mixed matrix membrane*

MOF – *Metal organic framework*

MP – *Multi-permselective*

NIPAM – *N-isopropylacry-lamide hydrogel*

NMR – *Nuclear magnetic resonance spectroscopy*

oHAB – *o-hydroxy-azobenzene*

PA – *Polyamide*

PANI – *Polyaniline*

PD – *Polydopamine*

PDMAEMA – *Poly(N,N-dimethyl aminoethyl methacrylate)*

PE – *Polyether*

PEBAx – *Poly(ether block amide)*

PEDM – *Copolymer consisting of PEGMA, PDMAEMA, and PMMA*

PEG – *Polyethylene glycol*

PEGMA - *Poly(ethylene glycol) methyl ether methacrylate*

PEI – *Poly-ethylenimine*

PG – *Pristine graphene*

P-GO-NF – *Polyether amine functionalized graphene oxide nano fluid*

PI – *Polyimide*

PMMA – *Polymethyl methacrylate*

POP – *Porous organic polymer*

PSf – *Polysulfone*

PVAm – *Polyvinyl amine*

RFG – *Recycled flue gas*

rGO – *Reduced graphene oxide*

S-GO – *Sulfonated polymer brush functionalized graphene oxide*

SPEEK – *Sulfonated poly(ether ether ketone)*

TMC – *Trimesoyl chloride*

UNFCCC – *United Nations Framework Convention on Climate Change*

vdF – *van der Vaals*

ZIF – *Zeolitic imidazole framework*

1. Introduction

1.1 Motive and object

The motive for this thesis is the necessity of climate prevention. Rapid economic growth has contributed to an increasing demand for energy, and a distinct consequence is the escalating in the use of conventional fossil fuels, like coal, oil, and natural gas, that have become the key energy sources since the industrial revolution.[1] Fossil fuels provide 81% of the world's commercial energy supply, however, fossil fuels have an adverse effect on the environment related to the emissions of the greenhouse gas CO_2.[2] Annual global emissions of CO_2 have intensified by approximately 80% between 1970 and 2004, and the average world temperature is expected to rise by 6,4% during the twenty-first century.[3,4]

The repercussion of global warming can be witnessed in the severity of tropical storms, ocean acidity, the rising of sea levels, because of glacier melting, as well as regionally uncommon droughts, floods and heat waves, resulting in destruction of ecosystems.[4,5] The worsening climate situation due to global warming has therefore become a widespread public concern where collaborative programs such as Intergovernmental Panel on Climate Change (IPCC) and international agreements like United Nations Framework Convention on Climate Change (UNFCCC) have been established. These programs have a goal to develop and improve strategies to reduce atmospheric concentrations of greenhouse gases, and amongst these initiatives is carbon capture and storage (CCS), which has gained significant attention during the last years.[3]

The capture and sequestration of CO_2 is a central strategy for making fossil fuel energy more competitive, as it offers the opportunity to meet increasing demands for fossil fuel energy in the short- to medium-term, whilst reducing the associated greenhouse gas emissions line with global targets.[3,6] CCS has shown promising results, and may contribute to reduce the CO_2 emissions by approximately 85-90% from large point emission sources.[1] Norway has through decades experimented with CO_2 separation in the petroleum industry, but despite being available for many years, CCS technology has not been widely deployed. The main reasons for the slow break through, are the high energy penalty and costs related to the implementation. It is therefore necessary to develop well-functioning technologies that can meet the energy penalties and the related economic challenges.

1.2 Carbon Capture and Storage (CCS)

The basic concept of CCS is to capture CO_2 prior to its release into the atmosphere. High-density CO_2 generated by emission sources is captured, compressed, transported, and then either reutilized industrially or stored permanently.[1,4] The storage of CO_2 often includes depositing it safely underground or in an ocean-bedrock sediment layer, whilst the capture of CO_2 can be achieved by three different methods: post-combustion, pre-combustion and oxy-fuel combustion.[4]

1.2.1 Post-combustion

In post-combustion existing power plants use air for combustion and generate a flue gas at atmospheric pressure.[6] The flue gas contains a relatively low concentration of CO_2 (5-25%), and small amounts of sulfur dioxide (SO_2), nitrogen dioxide (NO_2), and oxygen gas (O_2). The separation of the diluted, low pressure CO_2/N_2 mixture is therefore a major challenge, where a large volume of gas is needed. This means large equipment sizes and high capital costs.[7] Separation can be done in several ways, but the low concentration of CO_2 may affect the capture efficiency, the energy penalty, and the associated costs for reaching the ideal concentration needed for transporting and storage.[8,9] Advantages include a retrofit-friendly strategy, and the lower total electricity cost compared to other alternatives.[7] (Fig 1.1)

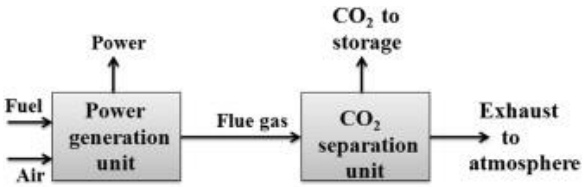

Figure 1.1: Principle of post-combustion in CO_2 capture.[7]

1.2.2 Pre-combustion

In pre-combustion the flue gas is pre-treated before combustion. This involves a partial oxidation reaction through a gasification process under low oxygen level, forming a syngas consisting of carbon monoxide (CO) and hydrogen gas (H_2).[8] The syngas is normally free from other pollutant gases, and will undergo a steam reforming hydrocarbons followed by a water-

gas shift reaction. The water-gas shift reaction converts the CO into CO_2, making a higher concentrated CO_2 flue gas mixture to facilitate the separation.[7]

$$\text{Coal} \xrightarrow{\text{gasification}} \text{CO} + \text{H}_2 \tag{1.1}$$

$$\text{CO} + \text{H}_2\text{O} \xrightarrow{\text{water-gas shift}} \text{CO}_2 + \text{H}_2 \tag{1.2}$$

$$\text{CH}_4 + \text{H}_2\text{O} \xrightarrow{\text{reform}} \text{CO} + \text{H}_2 \tag{1.3}$$

After separation CO_2 is transported and stored, while H_2 is used to generate power before being released into the atmosphere. The main disadvantage with this method is that it requires a chemical plant for the pre-treatment part, which few plants have, and this results in high capital and operating costs. Advantages are that the high CO_2 concentration enhances sorption efficiency of the separation unit and reduces the energy capture penalty of the process.[7,9] (Fig 1.2)

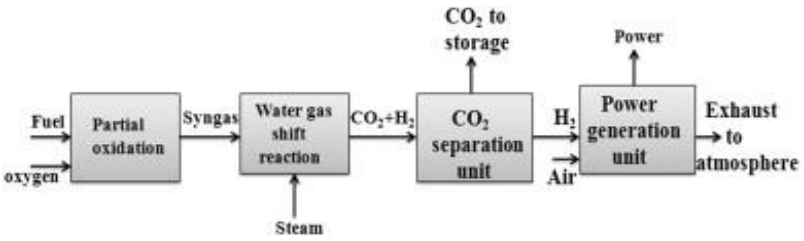

Figure 1.2: Principle of pre-combustion in CO_2 capture.[7]

1.2.3 Oxy-fuel Combustion

Oxy-fuel combustion consists of a cryogenic air separation unit that supplies high-purity oxygen to the power generation unit before combustion. The fuel is burned in nearly pure oxygen (95%), and amounts of NO_x -gases are heavily reduced compared to the other two methods.[8] Prior the combustion a recycled flue gas (RFG) is added to the generation unit.[7] The gas steam after combustion mainly contains CO_2 and water vapor, where the water can be easily removed by condensation, and the purified CO_2 can be transported and stored. The challenges

in this method are the additional air separation unit required and the RFG-recirculation system which increase the cost, making this method not considered economically beneficial. (Fig 1.3)

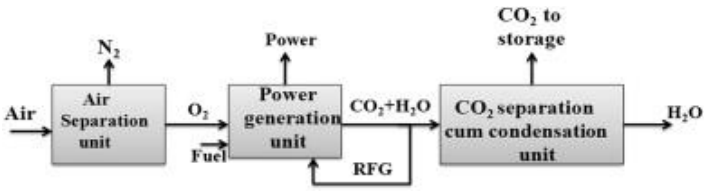

Figure 1.3: Principle of oxy-fuel combustion in CO_2 capture.[7]

1.2.4 Separation Technique

There are several techniques to isolate the CO_2 from the flue gas steam prior transportation. Separation can be done by absorption, adsorption, cryogenic separation, membrane separation, gas hydrates, and chemical looping.[3] (Fig 1.4)

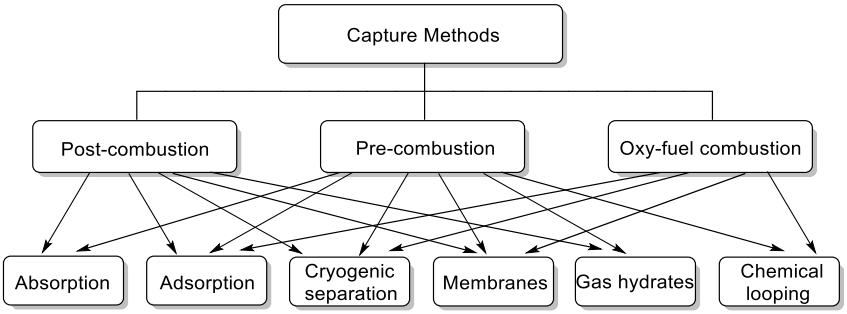

Figure 1.4: Materials for CO_2 capture in the context of post-combustion, pre-combustion, and oxy-fuel combustion.[3]

This thesis is mainly focused on post-combustion processes as they seem to be the most retrofit-friendly method. For the isolation of CO_2 gas, membrane-assisted separation will be the central technique. Membranes operate as a filter, and may consist of different materials, each with distinct properties. Mixed matrix membranes (MMM) are attractive, as they consist of a polymeric matrix that is incorporated by other materials enriching its properties. These additive nanofillers can consist of a multitude of materials.

Recently, ionic liquids (ILs) have been identified as good CO_2 capturing medium due to high solubility, which can be attributed to the reversible interactions between CO_2 and nitrogen

atoms present in IL ions.[10] These interactions with CO_2, also effectively increase the sorption kinetics. Another promising material are the metal organic frameworks (MOFs), which is a hybrid material consisting of an inorganic unit (i.e. metal ions or clusters) and an organic linker.[11] The material has shown great potential as nanofillers in polymer membranes, because of the crystalline structure with properties like high porosity with customizable pore sizes, and large surface area. Due to the partially organic character, and a surface area that can easily be functionalized, the material offers good connection between the nanofillers and the polymer chains, which results in a good dispersion and helps optimizing the gas separation.[12] Zeolitic imidazolate frameworks (ZIFs) are a sub-category of MOFs, formed by using Cu or Zn as the inorganic metal clusters and imidazole as the organic linkers. This class of materials has shown improved thermal, chemical and moisture stability, compared to MOFs, making it an attractive nanofiller in mixed matrix membranes.[13] Other common nanofillers are carbon nanotubes (CNTs), which are graphitic carbon sheets rolled into a tube cylinder. CNTs have good mechanical properties, thermal stability and internal cavities which facilitate gas transport, hence being suitable for this type of application.[14] Silica nanoparticles are another variant of inorganic fillers for MMMs and can be divided into non-porous silica particles and meso-porous silica particles. The non-porous materials do not engage in the gas transport directly, but change the packing of the polymer chains, consequently improving the permeability and selectivity. The meso-porous materials have inherent pores and have shown good separation performance.[15]

Despite that these materials have shown promising results, they often exhibit shortcomings regarding selectivity. This thesis will focus on mixed matrix membranes incorporated by graphene-based materials which is a relatively new class of materials in these applications. Graphene is a material that possesses unique qualities such as high thermal conductivity, high fracture strength and high Young's modulus, and exhibiting a high quantum Hall effect.[16] Moreover, graphene also has a large surface area which can easily be functionalized by other organic functional groups, enriching the properties of the final MMM.[17] The strong material has gained an ever-increasing interest during the last years and seems to be an attractive candidate for incorporation in polymeric membranes.

1.3 Aim of the Thesis

This thesis was part of an ACT-ERANET project on "Innovative membrane systems for CO_2 capture and utilization at sea – MemCCSea". Originally, the scope was to synthesize different materials bearing moieties that have shown promising results for CO_2 capture, and aromatic anchoring groups, i.e. pyrene, for non-covalent attachment onto graphene. Once the nano-ensembles were prepared they would be sent to our collaborators at the National Energy Technology Laboratory (NETL, USA), in order to disperse them into a poly-vinylamine matrix and measure its performance for CO_2 capture. The literature is virtually non-existent for these types of materials. Synthetic approaches were designed to synthesize the organic addends and characterization techniques to study the decorated graphene ensembles were available. Considering the dispersion of the graphene nano-ensembles into a polymer matrix, the plan was also to explore different chain lengths of the anchoring group (pyrene) *vs* the functional units. In addition, as a side project to conclude a holistic approach to the problem we worked together with a co-student with on her project on covalently functionalized graphene hybrids. The comparison of the covalent *vs* non-covalent approach would be compared in MMMs and provide useful insight. However, due to global COVID19 outbreak and the limited experimental time, it was decided to shift the project into a theoretical-based master's thesis for comprehensive review of current progress for graphene hybrids in carbon capture and storage (CCS).

The goal of this thesis is therefore to present recent published literature regarding functionalized graphene-based nanomaterials and their performance as additives in polymeric membranes. Analyses, evaluation, and performance in CO_2 capture membranes is given. Through the view of a synthetic chemist, we try to focus on identifying which components/functional groups, decorating graphene, can effectively increase the performance of the CO_2 capture membranes in order to guide future synthetic attempts on the project. As the performance and the chemistry on graphene is heavily dependent on the chemical composition of the polymer matrix used, we opt to structure the thesis by membrane type, in order to facilitate the interested reader. The originally designed syntheses will also be presented as a work for future investigation.

1.4 Overview

The introduction presented the motive for the thesis, in addition to give a short introduction of carbon capture and storage, before presenting the aim of the thesis. In the theoretical review, relevant theory regarding membranes and graphene-based materials will be presented, including some functional units and their beneficial features. For the literature research part, the performance of different reported membranes will be analysed and compared, before a conclusion summarizes the most interesting results and discovered trends. At the end, there will be a work in progress chapter, where the originally planned work will be presented. This includes organic synthesis theory along with details regarding the reactions and mechanisms performed in the lab before the lock-down, followed by the experimental part.

2. Theoretical Review

In this chapter, the theoretical basis of the thesis will be presented involving general theory of membrane separation and relevant graphene chemistry, along with a description of possibly functional units and their features.

2.1 Membrane Technology

Membranes are advantageous due to manufacturing scalability, low costs, energy efficiency, and small footprints.[18] A membrane performs as a filter allowing certain molecules to permeate through, while blocking other molecules.[19] (Fig 2.1) The selectivity of different gases may result from differences in the affinity to the membrane material, or simply differences in molecular sizes, molecular weights, etc. For carbon capture, a membrane should satisfy certain requirements such as having high CO_2 permeability, high CO_2/N_2 selectivity, thermal and chemical resistance, aging resistance, as well as being cost effective.[8,19]

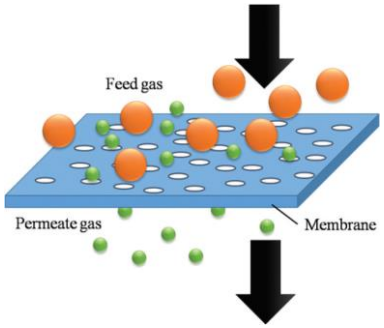

Figure 2.1: Schematic representation of membrane separation for gas mixtures.[19]

The permeability of a membrane depends on both the solubility and the diffusivity in the membrane, and can be expressed by the equation:

$$P = S \times D \tag{2.1}$$

where P is the permeability, S the solubility, and D the diffusivity. However, a more common unit for gas permeability used in membrane technology is Barrer, which measures the rate of

fluid flow passing through an area of material with a certain thickness driven by a given pressure.[20]

$$1\ \text{Barrer} = 10^{-10}\ \frac{\text{cm}^3_{\text{STP}} \cdot \text{cm}}{\text{cm}^2 \cdot \text{s} \cdot \text{cmHg}} \tag{2.2}$$

Another expressed unit is the Gas Permeance Unit (GPU),[21] which can be expressed as the ratio of the permeability with the thickness of a membrane:

$$1\ \text{GPU} = 10^{-6}\frac{\text{cm}^3_{\text{STP}}}{\text{cm}^2 \cdot \text{s} \cdot \text{cmHg}} \tag{2.3}$$

Selectivity of a membrane on the other hand, is defined as the ratio of the permeability of given gases:

$$S = P_A / P_B \tag{2.4}$$

where S is the selectivity, and P_A and P_B are the permeabilities of the component gases A and B, respectively. In order to determine the efficiency of a membrane both permeability and selectivity need to be considered. Unfortunately, high permeability generally gives poor selectivity. This trade-off was first established by L. M. Robeson, and has been accepted as a general trend, forming the Robeson upper bound 2008.[22] (Fig 2.2)

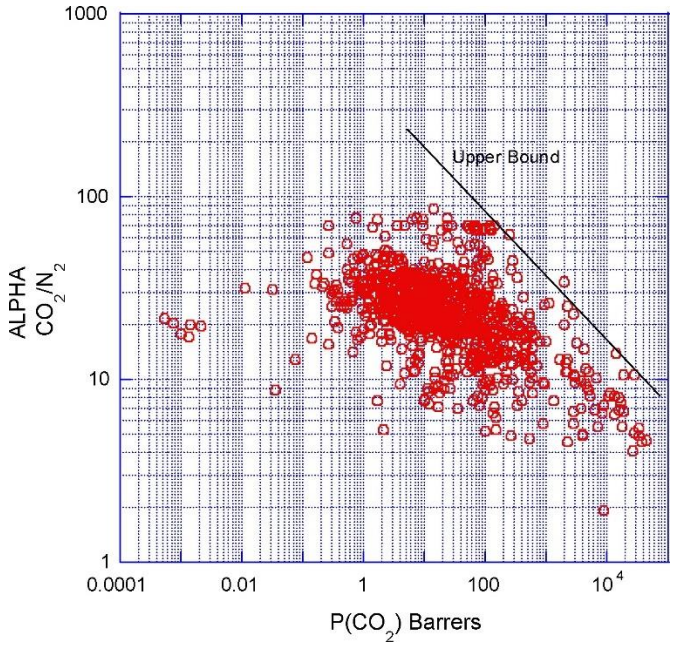

Figure 2.2: Robeson upper bound (2008) for CO_2/N_2 separation, where membranes surpassing the upper bound is desired and considered high-efficient.[22]

In post-combustion the flue gas contains CO_2 and N_2, and this separation mainly relies on surface diffusion and solution diffusion, which is driven by the differences in adsorption-ability and solubility between the gases. Furthermore, the diameter of CO_2 is slightly smaller than that of N_2, which enhances the diffusion of CO_2.[19] The major challenge in the separation is the low concentration of CO_2 in the flue gas, and this results in low driving force of CO_2 permeation. The high temperature of the gas will also rapidly destroy the membrane, so the gas must be cooled below 100 degrees prior the separation.[6] However, there are different materials being used in membranes, each with distinct properties.

2.1.1 Mixed-matrix Membranes

Mixed-matrix membranes are polymeric matrices (continuous phase) incorporated with a inorganic (most commonly) material (discrete phase) in the form of micro- or nanoparticles.[23,24] The use of two materials with different selectivity and flux offers enhanced properties.[25] The permeability of a gas through a nanoparticle-filled polymeric membrane depends on the intrinsic properties of the nano-filler and the polymer. The CO_2/N_2 selectivity is expected to improve owing to the zig zag passages created within the membrane, where the tortuous channels will favour the smaller sized CO_2 molecules to diffuse through the membrane, while hindering diffusion of the relatively larger N_2 molecules.[26] (Fig 2.3)

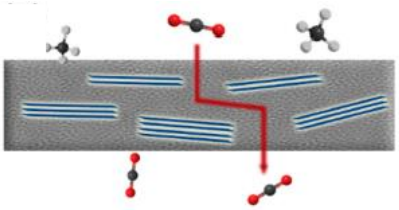

Figure 2.3: Schematic representation of a mixed-matrix membrane; allowing CO_2 to permeate while CH_4 gets blocked.[24]

2.2 Graphene as Nano-fillers

Addition of inorganic materials as nano-fillers offers improved properties for aggressive environments and helps stabilize polymer membranes.[27] Graphite is a three-dimensional sp^2-hybridized material and consists of stacked layers of graphene. The graphene layers interact through weak van der Waal's (vdW) forces and can be exfoliated into two-dimensional sp^2-

hybridized carbon sheet arranged in a hexagonal monoatomic honeycomb lattice.[28,29] There is a certain disparity in nomenclature: *pristine graphene* (PG) is considered to be perfect, defect-free single-layered graphene. Derivatives comprising of less than ~10 layers are commonly referred to as graphene or, more accurately, as *few-layered graphene* (FLG). Another variant, referred to as *graphene oxide* (GO), refers to graphene that is being heavily decorated by oxygen-containing groups. This material can also be reduced, with the use of various reducing agents, yielding reduced graphene oxide (rGO).

All these structures have strong and flexible bonds between the carbon atoms, giving the materials thin, strong, and stiff qualities. Other properties include unique electronic and mechanical features like high thermal conductivity, high fracture strength, high Young's modulus, and a high quantum Hall effect.[29,30] Due to these diverse properties, graphene has potential for a great number of applications, one of which is being an attractive candidate as a nano-filler in gas sorption and separation.

Graphene also possesses a high aspect ratio. The use of this material as a nano-filler will therefore increase the length of the path of gas diffusion, as well as reduce the mobility of polymer chains in the polymer matrix.[31,32] This has a positive effect for the gas diffusion selectivity, restricting the diffusion of larger molecules and favouring the diffusion of small molecules with less resistance, like CO_2 molecules.[32] (Fig 2.4)

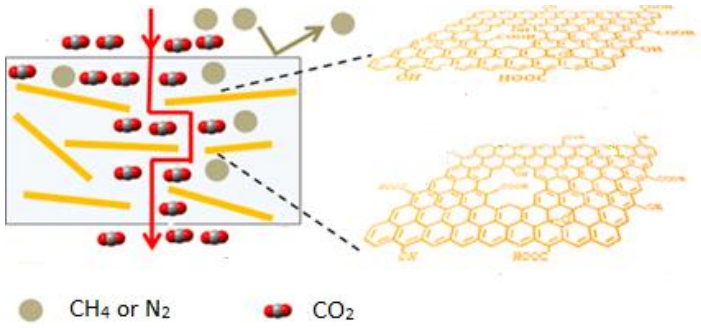

Figure 2.4: The schematic of a mixed-matrix membrane, separating CO_2 and CH_4/N_2 using graphene-oxide nanosheets incorporated in the membrane.[33]

2.2.1 Production of Graphene-based Materials

Due to graphene's promising and diverse properties, there has been an increase in attention towards the material, contributing to a development of a multitude of approaches for obtaining high quality material on a large scale.[34] This includes approaches such as mechanical exfoliating, epitaxial growth, oxidation and subsequent reduction, and solvent exfoliating.

2.2.1.1 Mechanical Exfoliation

Mechanical exfoliation can be described as repeated peeling of small mesas of highly orientated pyrolytic graphite.[35] This can be done in two ways: (A) using a normal force, numerous times, peeling off graphitic layers until, one eventually, ends up with single-layer graphene, or (B) using a shear effect, where unbalanced lateral compressive stress separates two adjacent flakes.[36] (Fig 2.5)

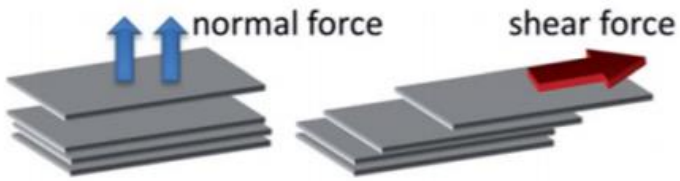

Figure 2.5: The two mechanical routes for exfoliating graphite into graphene flakes using normal force and shear force.[36]

2.2.1.2 Epitaxial Growth

Epitaxial growth is a process where epitaxial graphene (EG) sheets are grown by thermal decomposition on the surface of SiC.[37] At high temperatures, Si atoms starts to evaporate from the surface, causing the C atoms to segregate on the surface to form C-rich surface layers. These layers range from the interfacial graphene layer, to single-layer EG, bi-layer EG, and few-layer EG.[38] (Fig 2.6)

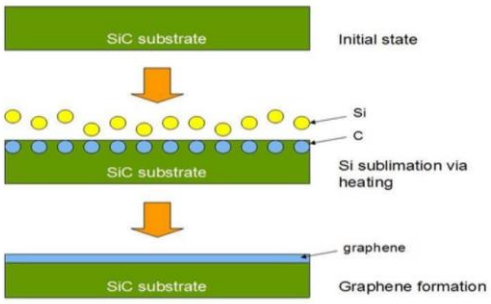

Figure 2.6: Illustration of epitaxial growth on a SiC substrate, resulting in epitaxial graphene driven by thermal decomposition.[38]

2.2.1.3 Oxidation and Reduction

Producing graphene oxide involves using natural graphite as the start material, which is treated with strong oxidizing agents in highly acidic media to introduce the oxygen functional groups. These incorporations separate and weaken the weak interactions between the graphitic layers resulting in graphene oxide.[39] The most commonly used method is the Hummers' method, which involves addition of potassium permanganate, sodium nitrate, and sulfuric acid to graphite.[40] In order to obtain the reduced graphene oxide, GO must undergo a reduction process which can be thermal or chemical. Thermal-assisted reduction can take place *via* annealing, microwave irradiation or photo reduction, while chemical reduction can take place *via* chemical reagent reduction, photocatalyst reduction, electrochemical reduction or solvothermal reduction.[41] (Fig 2.7)

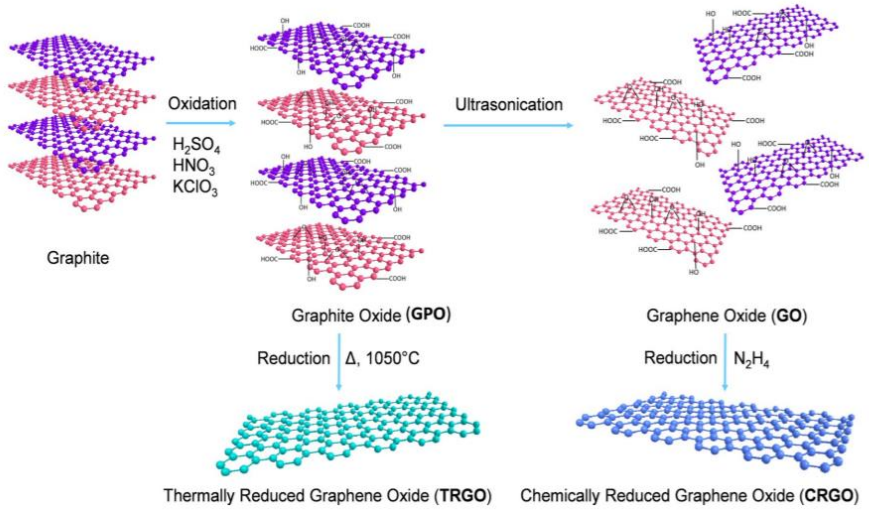

Figure 2.7: Schematic representation of chemically modified graphene preparations.[39]

2.2.1.4 Solvent Exfoliation

Solvent exfoliation as the name suggest involves the solvent-assisted exfoliation of graphite by the use of sonication to obtain few-layered graphene.[42] (Fig 2.8) Using this method involves graphite flakes being sonicated in an organic solvent (e.g. *N*-methyl-2-pyrrolidone, 1,2-dichlorobenzene or several other exfoliating agents), followed by a purification of the exfoliated particles from unreacted graphite by centrifugation. The resulting supernatant contains a graphene dispersion.[43] Depending on the centrifugation process, the graphite quality can be tuned, resulting in few-layered graphene or single-layered graphene, by varying the centrifugal force applied. This method is one of the most promising, as it seems to be the simplest approach to prepare dispersible graphene sheets on a large scale, at a low cost.[44] However, during the ultra-sonication process, some lattice defects will inevitably occur situated mostly at the edges due to breaking of larger graphite flakes into smaller nanoparticles.

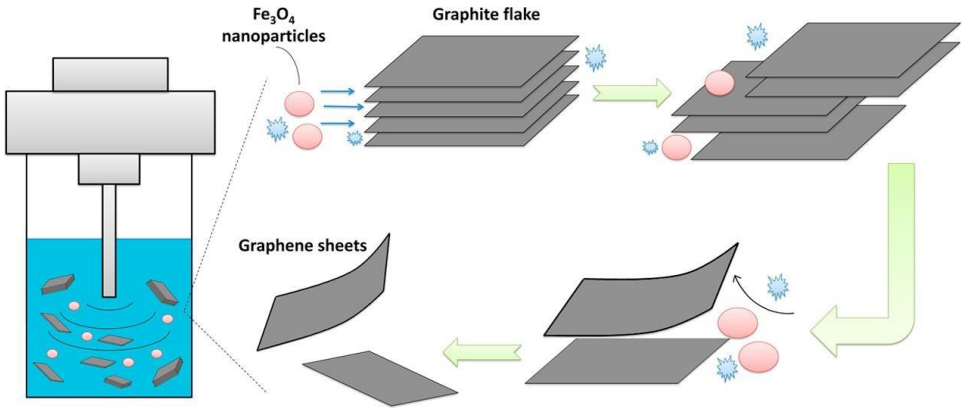

Figure 2.8: Schematic illustration of Fe_3O_4 solvent-assisted exfoliation of graphite, by the use of sonication to produce graphene dispersion.[44]

2.3 Functionalization of Graphene

Graphene does not possess any inherent affinity towards polymer membranes and is likely to create aggregates due to the strong π-π interactions between the graphene sheets, once introduced into the matrix. This inhibits the performance of the membrane and lowers its overall mechanical properties.[45] In order to optimize and facilitate graphene's incorporation and dispersion in a mixed matrix membrane, the sheets can be functionalized. Chemical functionalization of graphene is a highly attractive research area, due to graphene's large surface area which easily can be decorated by organic functional units.[46] The main purpose of

the functionalization is to get dispersibility of graphene in common organic solvents, which usually is obtained after attachment of certain organic groups as they lend their solubilization properties, offering improved stability and processing of graphene nanoparticles.[34] Obtaining dispersibility is crucial for the membrane mixing, and in most cases the introduction of nanofillers introduces new properties for the membrane, allowing possible enhancements such as improved diffusivity, solubility and reactivity selectivity to be achieved.[33,46]

The presence of ethylene oxide (EO) groups in membranes has been shown to achieve better CO_2/gas selectivity because of the excellent affinity EO groups possess for polar gases like CO_2.[47] CO_2 is also considered an acid gas, meaning that when dissolved in water it forms an acidic solution. This makes basic groups, such as amino groups, good as CO_2 carriers.[48] Since the reactions between CO_2 and amino groups are reversible in the presence of water, the reactivity selectivity of the membranes improve by increasing the content of amino groups.[49] The nitrogen functionalities are essential in the sorption capacity, since each mole of amine are able to capture 0.5 mole of CO_2. The reactions are reported as follows:

$$2CO_2 + 2RNH_2 + H_2O \rightleftharpoons RNHCOOH + RNH_3^+ + HCO_3^- \quad (2.1)$$

$$2CO_2 + 2RR'NH + H_2O \rightleftharpoons RR'NCOOH + RNH_3^+ + HCO_3^- \quad (2.2)$$

$$CO_2 + RR'R''N + H_2O \rightleftharpoons RR'R''NH^+ + HCO_3^- \quad (2.3)$$

Figure 2.9 illustrates the same schematic as Figure 2.4, except that EO-groups and amino groups are attached increasing the permeation for CO_2.

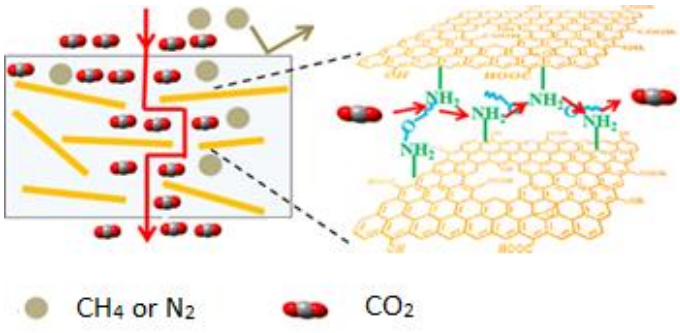

Figure 2.9: The schematic of a mixed-matrix membrane using amino-functionalized graphene-oxidized nanosheets as the inorganic incorporation in the membrane.[33]

There are two ways to insert functional groups onto the graphene nanosheet surface via chemical routes; by covalent and non-covalent functionalization.

2.3.1 Functionalization by Covalent Bonding

Covalent attachment creates covalent bonds by converting sp^2 orbitals into sp^3 orbitals, and can be achieved by the formation of covalent bonds between radicals or dienophiles and the carbon-carbon double bonds in graphene.[46] The aromatic character is then perturbed, and graphene can become a more stable and robust hybrid material.[50] The attachments can be performed through various routes involving: 1,3-dipolar cycloaddition, zwitterion cycloaddition, nitrene addition, nucleophilic addition, radical addition, click chemistry, hydrogenation, and a cyclopropanation (Bingel reaction).[34] There are also a multitude reaction pathways for covalent functionalization of graphene oxide.[50] (Fig 2.10)

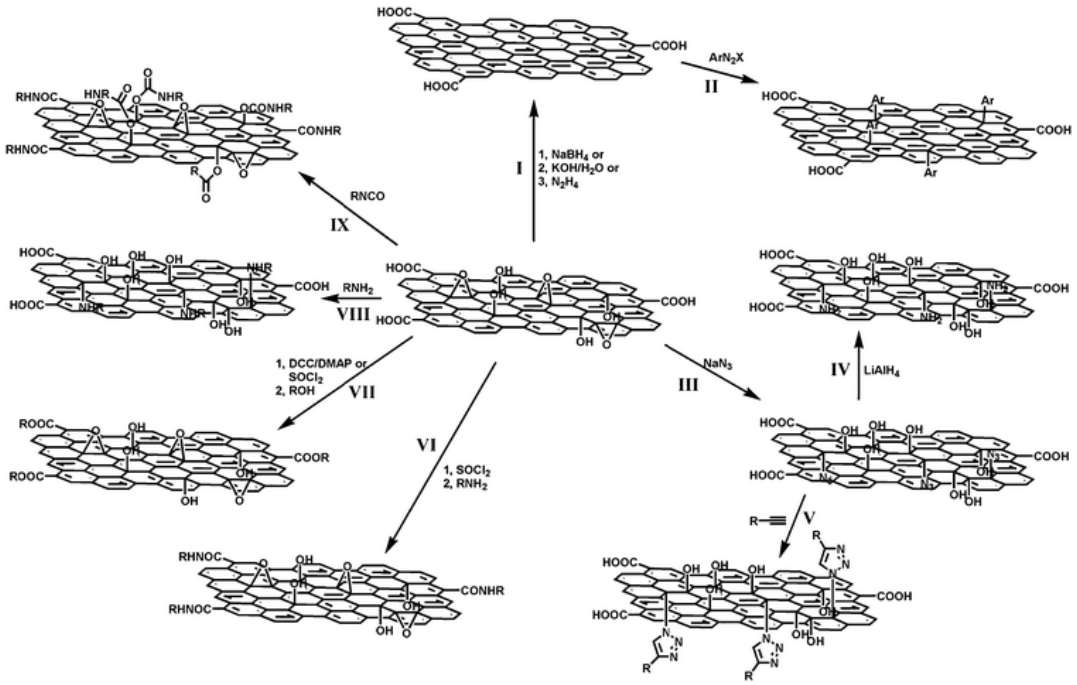

Figure 2.10: I) Reduction of GO by different approaches forming rGO. II) Covalent surface functionalization of rGO *via* a diazonium reaction. III) Reactions between GO and sodium azide, forming azide functionalized GO. IV) Reduction of azide functionalized GO proceeding amino-functionalized GO. V) Functionalization of azide-GO through click chemistry using R−C≡CH. VI) Acylation reactions between carboxyl acid groups and alkylamines, forming GO modified by long alkyl chains. VII) Esterification of GO through acylation reactions between carboxyl acid groups and alkylamines. VIII) Nucleophilic ring-opening between epoxy groups and amino groups. IX) Treatment with organic isocyanates resulting in derivatization of all carboxyl and hydroxyl groups *via* formation of amides and carbamates esters.[50]

2.3.1.1 Bingel Reaction

This reaction is a cyclo-propanation which, originally, was used in fullerenes (C_{60}). Diethyl bromo-malonates reacted with C_{60} in the presence of a strong base (often using 1,8-diazabicycloundec-7-ene, DBU).[51] The steps for the mechanism involved were as follows: (a) the base abstracting the acidic proton of the malonate derivative generating a carbanion or enolate, (b) the carbanion attacking the fullerene nucleophilically forming a new carbanion with the charge localized at the cage, (c) the bromide displacing in a nucleophilic substitution SN_2 reaction, causing an intramolecular ring closure.[52,53] (Fig 2.11)

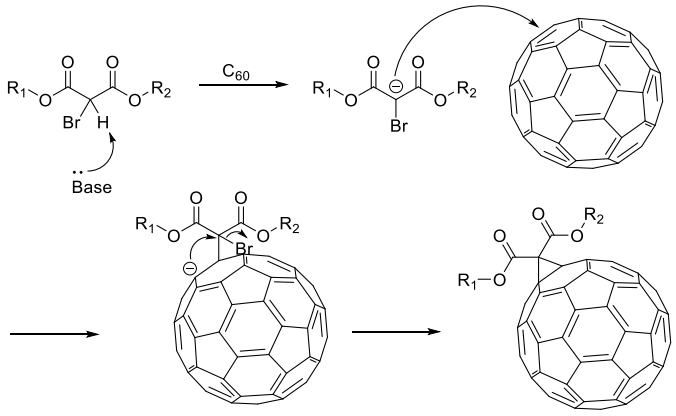

Figure 2.11: Bingel reaction mechanism for functionalizing fullerene.[52]

Unfortunately, the preparation of bromomalonates is complicated, and the yields are limited due to the simultaneous formation of dibromomalonates. The properties of these materials differ only slightly, making the separation almost impossible in many cases.[53] However, direct treatment of fullerenes with malonates in the presence of CBr_4 and DBU, can provide good yields, avoiding the problems associated with the separation of the bromomalonates derivatives.[53] This procedure can also be adopted in the functionalization of graphene, replacing the fullerenes with exfoliated graphene. Additionally, the reaction can proceed under microwave irradiation conditions, significantly, minimizing reaction times.[54] (Fig 2.12)

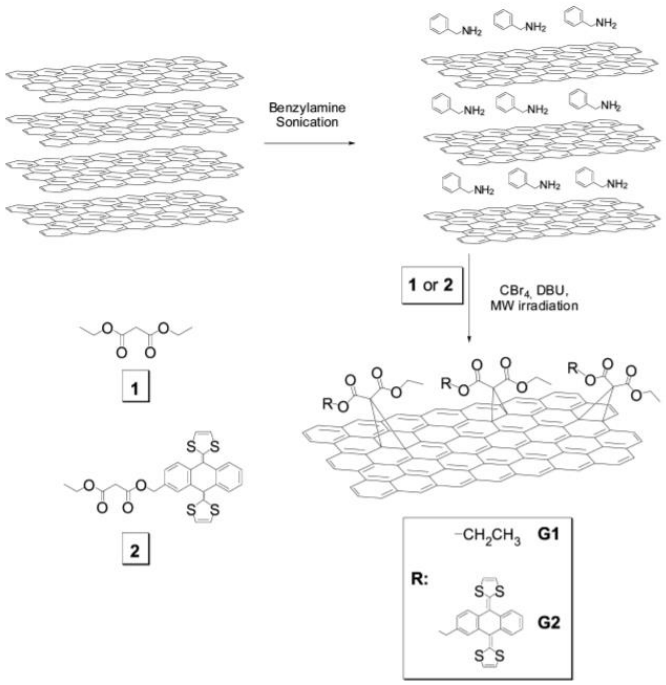

Figure 2.12: Preparation of functionalizing graphene using the Bingel reaction.[54]

2.3.2 Functionalization by Non-covalent Bonding

An attractive synthetic method for non-covalent functionalization is by taking advantage of intermolecular interactions involving π-systems, as it offers the possibility of attaching functional groups to graphene without chemically altering the structure or the electronic properties.[55] This proceeds through weak intermolecular interactions between the functionalizing molecule and the aromatic rings of graphene. Over the last two decades π-interactions in graphene sheets have been extensive studied, including gas–π interaction, H–π interaction, π–π interaction, cation–π interaction, and anion–π interaction.[56,57] The strength of these interactions is determined by attractive forces, being inductive, dispersive, and electrostatic interactions, and repulsive forces such as exchange repulsion.[57]

2.3.2.1 Non-polar Gas–π Interaction

In π-systems, when the counter-molecule is a polar molecule or a Lewis acid, both electrostatic and dispersion forces conduct the interaction. However, when the counter-molecule is a non-polar molecule, such as gas, dimers or hydrocarbons, only dispersion energies predominate.[58]

2.3.2.2 H–π Interaction

H–π interactions consist of hydrogen bonds. This involves molecules possessing a quadrupole moment, such as benzene, interacting with a permanent dipole, e.g. water.[59] The quadrupole moment provides substantial negative electrostatic potential for a favourable interaction with the protons of the water molecule. The polarizabilities of the π-electron systems are significant in governing the character and geometry, and the dispersion energy tends to correspond to the quantity of electrons participating in the interaction. In the case of extended π-systems, the multidentate H–π complexes are additionally stabilized by a significant contribution from the dispersion energy.[60] (Fig 2.13)

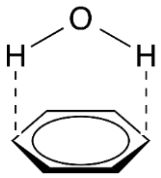

Figure 2.13: Protons in a water molecule interacting with the quadrupole moment of a benzene.[60]

2.3.2.3 π–π Interaction

π–π interaction, also called π–π stacking, refers to non-covalent interactions between aromatic rings in which the distance between the centroids is less than 7.0 Å.[61] Aromatic structures have π-systems with negatively charged and diffuse electron clouds, and exhibit attractive interactions predominated by dispersion when two systems possess similar electron densities.[59] Three geometry types are commonly observed regarding π–π stacking: (A) edge-to-face, (B) offset, and (C) face-to-face. (Fig 2.14)

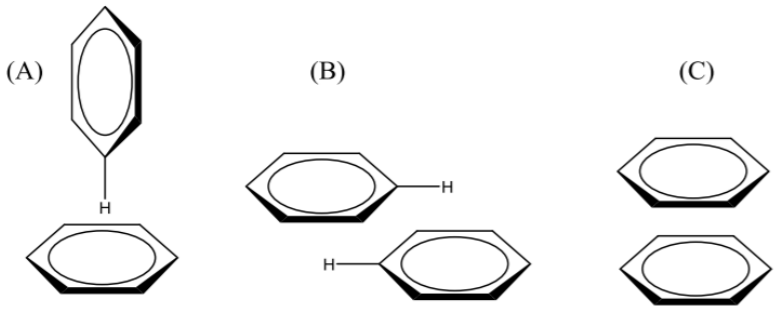

Figure 2.14: The different observed geometries for π–π stacking (A) edge-to-face, (B) offset, and (C) face-to-face.

2.3.2.4 Cation–π Interaction

This kind of interaction involves a positive charged cation interacting with an electron-rich π-system. The interaction can be surprisingly strong and has several potential applications in chemical sensors.[62] (Fig 2.15)

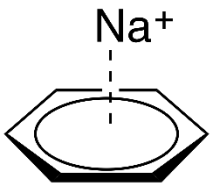

Figure 2.15: A sodium cation interacting with the π-system of a benzene.[62]

2.3.2.5 Anion–π Interaction

Anion–π interactions are very similar to cation– π interactions, only reversed, in which an anion interacts with an electron-poor π-system. In this case, the electron-poor π-system often consists of a conjugated molecule having electron-withdrawing substituents.[63] (Fig 2.16)

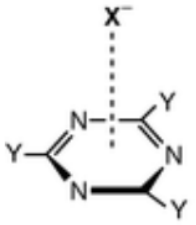

Figure 2.16: X^-, an anion (Cl^- or Br^-), interacting with a triazine substituted by withdrawing groups Y (F).[63]

2.3.2.6 Graphene–Ligand Non-covalent Interaction

Generally, there are a multitude of materials that can be employed in non-covalent functionalization synthesis, such as ionic, metallic or organometallic compounds (Al^{3+}, Mn^{2+}, CuO_2^{2-}, Fe_3O_4, $MnFe_3O_4^{2+}$) or ionic and poly-ionic liquids (polyvinyl imidazole, polyvinyl pyrrolidinone, triphenylenes, pyrene derivates). Various studies involving adsorbed molecules onto graphene surfaces have been conducted. Π-π stacking interactions are of a special interest because of the extended π-orbitals of graphene.

3. Literature Research

In this chapter, results from recent published literature regarding graphene-based materials used in mixed matrix membranes will be compared and analysed. There are different matrix materials, and it is therefore natural to categorize the results into matrix-based sections, making it easier to analyse the effect of certain functionalization groups. The matrices are PI, PEBAx, SPEEK, PSf, pEDM and EC.

3.1 PI-based MMMs

Polyimide (PI) is a polymer of imide monomers where the structure is commonly found as a part of a five- or six-membered ring. (Fig 3.1) This material has shown good potential as a membrane due to its mechanical properties, high thermal stability, and gas selectivity.[64] However, the permeability for CO_2 is relatively low which limits the application potential for CO_2 separation. Despite this, efforts have been made to fabricate novel polyimide membranes with high CO_2 separation performances.

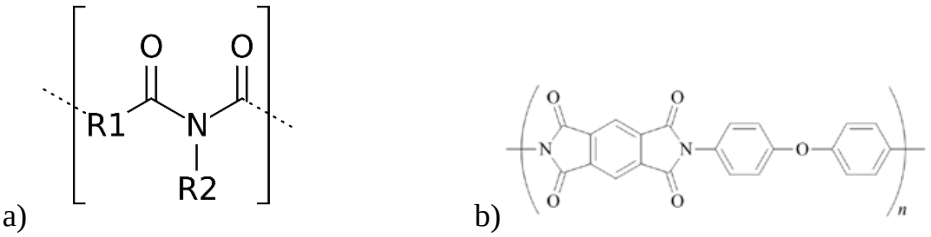

Figure 3.1: (a) The general structure of a polyimide, and (b) the structure of an example of a specific polyimide.[64]

Wang *et al.*[65] fabricated mixed matrix membranes by incorporating the zeolitic imidazole frameworks (ZIFs): ZIF-8 and ZIF-8 coated with polydopamine (PD) into PI matrixes. Other fabricated MMMs consisting of PI matrix, was generated by Gao *et al.*[66] who conducted hydroxyl functionalized ZIFs (ZIF-7-OH)/PI MMMs, and Sun *et al.*[67] who incorporated carbon nanotubes into PI matrixes. All these membranes showed relatively good CO_2 permeability, but rather poor CO_2/N_2 selectivity. Graphene has good aspects for facilitating a CO_2 selective

transport through the membrane and has therefore been tested as a novel incorporation into the PI matrix.

3.1.1 Performance of PI-based Membranes

Ge *et al*.[68] prepared aminated graphene oxide incorporated in a polyimide (PI) matrix. Aminated graphene oxide was obtained using mild ultrasonic exfoliation before fabricating the NH_2-GO/PI membrane using an *in-situ* polymerization approach. (Fig 3.2) The gas permeation tests were conducted at 15 °C using pure CO_2 and N_2 gases. Results indicated that the addition of NH_2-GO nanosheets significantly improved the CO_2 permeability and the CO_2/N_2 permeation selectivity of the MMMs. This was mainly due to the effective π-π stacking interactions between CO_2 molecules and the GO nanosheets, the interactions between CO_2 molecules and the amino groups on the GO nanosheets, and the polar bonds in CO_2 that had strong affinity to the polar PI polymer. Both permeability and selectivity increased when there was an increase in filler content up to 3 wt%. For higher nanofiller loadings, agglomeration of the GO nanosheets occurred in the matrix, making the polymer discontinuous and consequently decreasing its properties. The optimum loading of NH_2-GO was 3 wt%, reaching a permeability of 12.34 Barrer and a selectivity of 38.56.[68]

a) b)

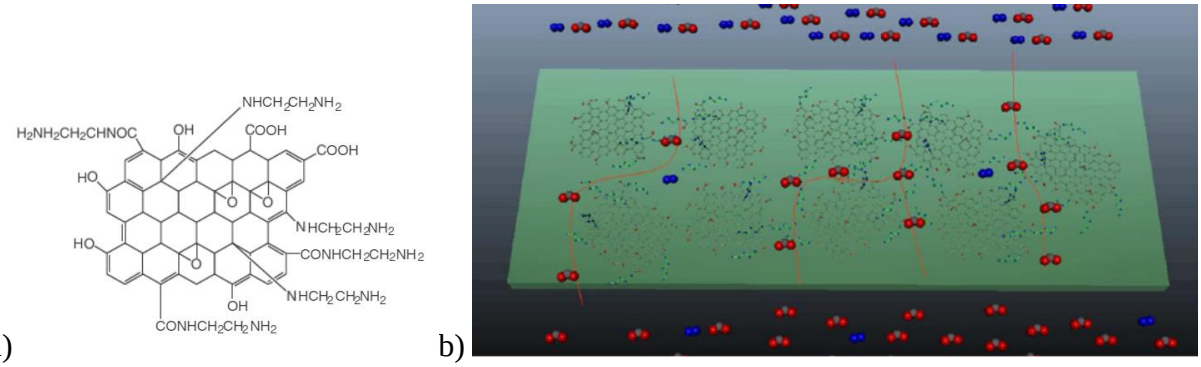

Figure 3.2: (a) Molecular structure of NH_2-GO, and (b) the gas transport mechanism of NH_2-GO/PI mixed matrix membrane.[68]

Another PI-based mixed matrix membrane was developed by Jia *et al*.[69] where the aminated metal organic framework (MOF), UiO-66-NH_2, was functionalized onto graphene oxide nanosheets, before incorporated into the PI matrix. Graphene oxide was synthesized by using the Hummers' method, and UiO-66-NH_2 was grown on the GO surface using an *in-situ* method,

before the nanocomposites were incorporated into the matrix using a solvent-assisted evaporation method. The nanoparticles were well-anchored on the GO nanosheets due to electrostatic interactions promoted by the functional groups. UiO-66-NH_2 possessed high porosity, good thermal stability, and a strong affinity towards CO_2 gas molecules due to the addition of amino-groups that effectively added a supplementary enhancement for the CO_2 affinity. (Fig 3.3)

Membranes with different filler loadings were prepared and tested with pure gases of CO_2 and N_2 at 25 °C and 3 bar. Pure PI held a CO_2 permeability of 2.28 Barrer and a CO_2/N_2 selectivity of 28.9, while a membrane prepared consisting of PI with a pure GO loading of 1 wt%, held permeability of 3.15 Barrer and selectivity of 64.3. There was a great enhancement for the selectivity, while a small increase in permeability was observed. The authors suggested that this was probably due to the non-existence of porosity in GO nanosheets, causing the gas molecules to only permeate through the edges of the sheets, increasing the selectivity for the smaller CO_2 molecules. By incorporating porous UiO-NH_2-GO, permeability increased gradually with an increase in the filler content, reaching 18.1 Barrer for a 20 wt% loading. However, CO_2/N_2 optimal selectivity was observed with filler content of 5 wt%, mostly because of to the occurrence of agglomeration of UiO-66-NH_2-GO particles when the filler content got higher. Agglomeration was presumably caused by the different physical properties between the nanofillers and the PI matrix. The best performance was therefore obtained using the MMM with 5 wt% loading of UiO-66-NH_2-GO, exhibiting a CO_2 permeability of 7.28 Barrer and a CO_2/N_2 selectivity of 52.0.[69]

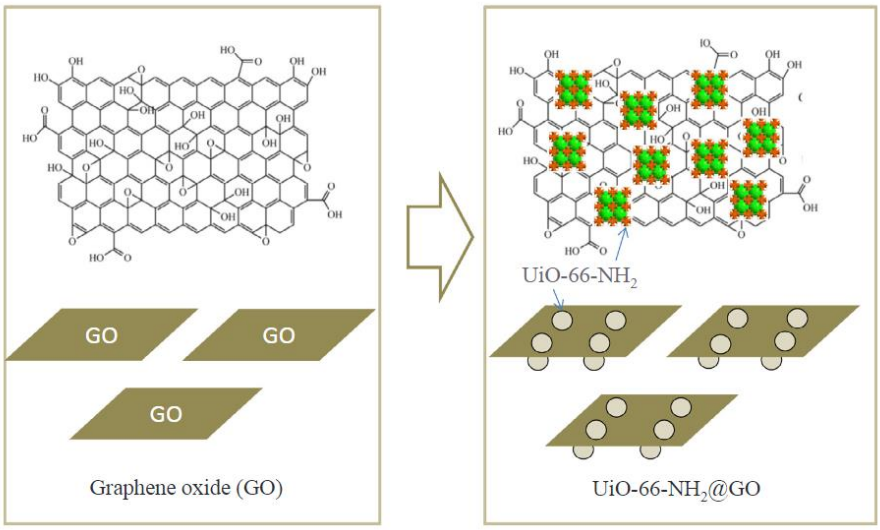

Figure 3.3: The fabrication of UiO-66-NH_2/GO nanocomposites.[69]

Wu *et al.*[70] modified mixed matrix membranes by incorporating PI matrix with polyethylene glycol (PEG) functionalized graphene oxide nanosheets. GO was synthesized by using the Hummers' method before PEG groups were attached, followed by incorporating the nanocomposites into a PI matrix *via* an *in-situ* polymerization. The introduction of PEG groups contributed to a higher gas diffusivity and offered good solubility for CO_2 gas molecules due to CO_2's quadrupole moment and favourable interaction with polar groups. (Fig 3.4) The modified PEG-GO nanosheets showed distinct results in selectivity for CO_2, correlated to the molecular weight of PEG on GO. Higher molecular weight caused increased polarity of the membranes, which contributed to higher solubility selectivity for CO_2. However, too much PEG functionalization caused impurities and formed agglomeration. For the loading content of PEG-GO in the PI matrix, both CO_2 permeability and CO_2/N_2 selectivity increased along with an increase, but eventually decreased due to agglomeration. The optimal filler content was therefore 3.0 wt%, achieving a CO_2 permeability of ~ 370 Barrer and a CO_2/N_2 selectivity of ~ 49.[70]

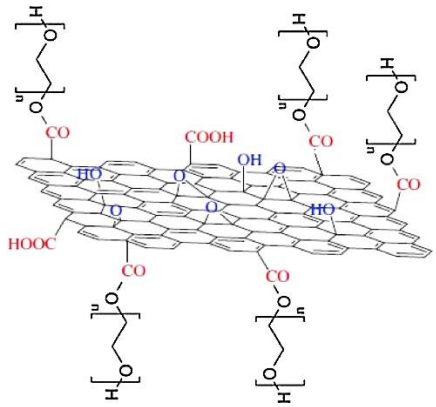

Figure 3.4: The molecular structure of PEG-modified GO.[70]

3.1.2 Compilation of Performances

As shown in Table 3.1, MMMs incorporated by ZIF-based nanofillers showed much better CO_2 permeability than the graphene-based nanofillers, due to the porous structures of ZIFs. However, N_2 permeability was also high, resulting in a low CO_2/N_2 selectivity. Thus, the GO-based nanofillers exhibited better selectivity, since the constructed zig-zag pathways through the membranes were beneficial for permeating predominantly CO_2 molecules. For the different functional units on graphene oxide, PEG showed best permeability whilst MOF showed best selectivity. It should be mentioned that the pure PI membranes used in the diverse experiments

did not inherent the exact same properties and showed distinct values for permeability. It was also unclear whether some of them were pre-treated with water prior the gas permeation tests or not, which should be clarified due to the impact water may have on the membrane's abilities.

Table 3.1: Comparison of CO_2 separation performance between PI-based mixed matrix membranes.

Filler content	Polymer	wt% loading (best MMM performance)	Test conditions	P_{CO2} (Barrer)	CO_2/N_2 selectivity
ZIF-8[65]	PI	20	Pure gas, 35 °C	896	16
ZIF-8-PD[65]	PI	20	Pure gas, 35 °C	702	18
ZIF-7-OH[66]	PI	14	Pure gas, 25 °C, 4.5 bar, dry state	273	38
CNTs[67]	PI	3	Pure gas, 15 °C, 1 bar, dry state	9.06	38
NH_2-GO[68]	PI	3	Pure gas, 15 °C, 1 bar, dry state	12.34	38.56
UiO-NH_2-GO[69]	PI	5	Pure gas, 25 °C, 3 bar, dry state	7.28	52.0
PEG-GO[70]	PI	3	Pure gas, 30 °C, 10 bar, humidified state	370	49

3.2 PEBAx-based MMMs

Poly ether-block-amide (PEBAx) is a thermoplastic elastomer, considered as a promising polymeric material applied in mixed matrix membranes for CO_2/N_2 separation.[71] The material consists of polyether (PE) segments as well as rigid blocks of polyamide (PA), where the PE segments are parts of alcohols whilst the PA blocks parts of carboxylic acids. The presence of polar moieties, such as ethylene oxide (EO) groups, in the polymer matrix offers high CO_2 solubility due to the dipole-quadrupole interactions between EO units and CO_2 molecules, being beneficial for the CO_2 selectivity. Moreover, PEBAx holds superior mechanical and dynamic properties. (Fig 3.5)

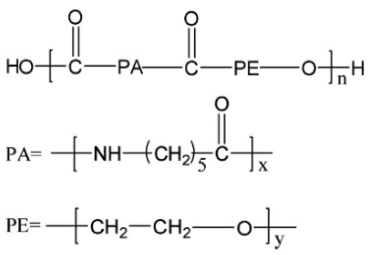

Figure 3.5: The structure of the polymeric material PEBAx.[71]

When measuring the performance of membranes, it can be done under dry or humidified conditions, conducting permeation experiments with pure- or mixed gas. Under humidified conditions water is present, which often results in an enhanced solubility selectivity for CO_2 if amino groups also are involved, owing to the reversible reactions between amines and CO_2. In this chapter, there will be presented performances of PEBAx-membranes under dry and humidified states, focusing on the membranes showing the best performances regardless of which gas feed is being used.

3.2.1 Performance of PEBAx-based Membranes at Dry State

Dai *et al*.[72] generated mixed matrix membranes composed of imidazole functionalized graphene oxide (Im-GO) and PEBAx matrix. (Fig 3.6) The incorporations of imidazole caused Lewis-acid Lewis-base interactions between the negatively charged oxygen atoms in CO_2 and the N atoms in the heterocyclic imidazole, facilitating the CO_2 transport in the membrane. Different Im-GO loadings of 0.2, 0.4, 0.6, 0.8, and 1.0 wt% were prepared as fillers and gave diverse results. A modest enhancement in CO_2 permeability was observed at low Im-GO doping, but the permeation decreased when the Im-GO loading got higher than 0.5 wt%. For the selectivity, there was a trend exhibiting a gradually increase with the increase in filler content. The loading of 0.8 wt% showed the best performance, holding a CO_2 permeability of 64.0 Barrer and a CO_2/N_2 selectivity of 90.3.[72] Moreover, the selectivity for CO_2/N_2 increased by 46% compared to the pristine PEBAx membrane.

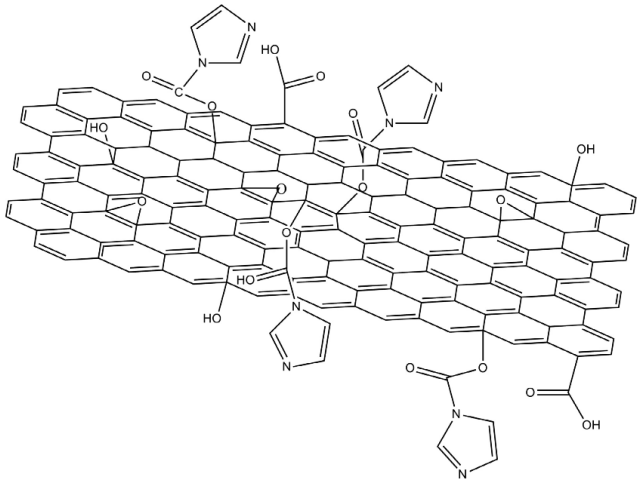

Figure 3.6: Schematic structure of imidazole functionalized graphene oxide, Im-GO.[72]

Cong *et al.*[73] combined a porous organic polymer (POP), based on *o*-hydroxy-azobenzene (oHAB), with graphene oxide for incorporation in a PEBAx matrix. (Fig 3.7) oHAB was synthesized under mild conditions using a diazonium coupling reaction, involving aryl-diamine and tris-phenol in water. The functional units were then loaded onto the graphene oxide surface, attaching through bonding effects, before incorporated into the PEBAx matrix using solvent evaporation. The structure of oHAB had a phenolic mesoporous character, where the azo-group rejected N_2 molecules, whilst the unreacted phenolic groups had a high CO_2-philic character. The presence of large amounts of phenolic hydroxyl groups gave the ability to form hydrogen bonds. Some *via* bonding effects with graphene oxide, causing oHAB to control the *d*-spacing, and others *via* hydrogen bonds with CO_2, increasing the affinity. Due to the tailoring of the interlayer space between the graphene oxide nanosheets, oHAB was able to enhance the CO_2/N_2 separation performance by constructing CO_2-philic channels. The best performance was achieved for oHAB-GO 10-2, where the 10-2 represent the relative mass proportions of oHAB and GO, respectively. The CO_2 permeability was found to be 696 Barrer, and the selectivity of CO_2/N_2 was 51.2, contributing to a result beyond the Robesabon's upper bond (2008).[73]

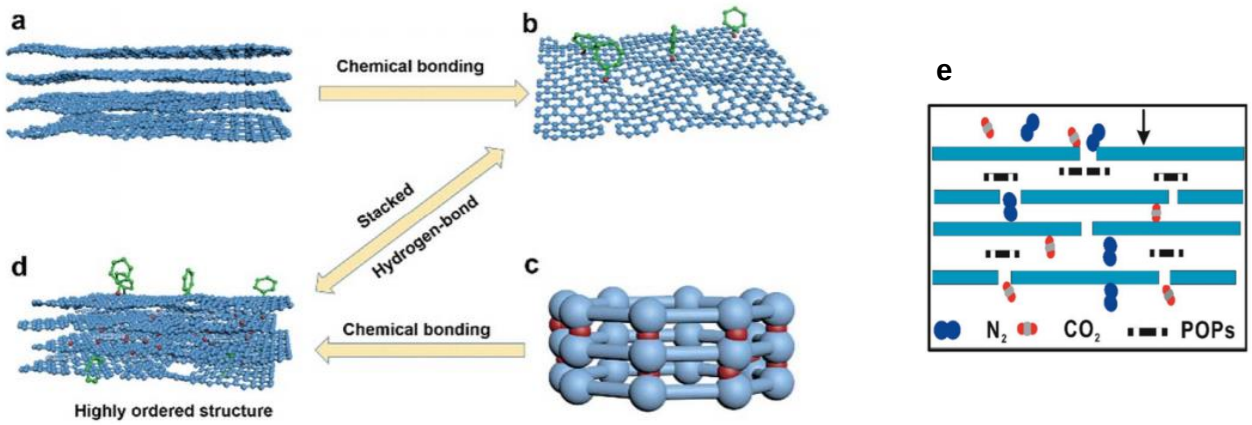

Figure 3.7: a) Graphene oxide, b) binding for graphene oxide and oHAB, c) stacked oHAB, where the light blue represents the oHAB rings and the red represent hydrogen bonds, d) the ordered stacking structure of oHAB and GO combined, e) schematic diagram of double-layered molecular sieve from ordered graphene oxide modified with oHAB.

Shawqi *et al.*[74] prepared mixed matrix membranes consisting of PEBAx incorporated by aminated partially reduced graphene oxide (A-prGO) nanosheets, fabricated on top of a supporting poly-sulfone layer. Membranes were prepared with different nanofiller loadings of 0, 0.05, 0.1, 0.2, and 0.6 wt%. High filler loadings caused aggregation between the nanosheets,

resulting in a poorer CO_2 selectivity. The best performance was obtained using the membrane with 0.1 wt% filler content, achieving a CO_2 permeability of 47.5 Barrer and a CO_2/N_2 selectivity of 105.56, reaching above the Robeson upper bond (2008).[74] (Fig 3.8)

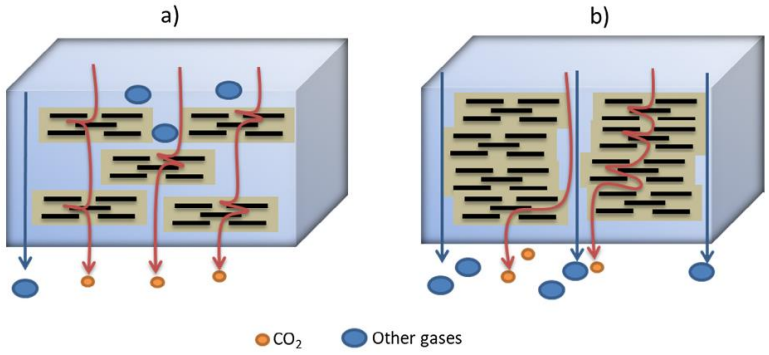

Figure 3.8: a) An illustration of optimum loading of A-prGO, and b) an illustration of excessive loading of A-prGO.[74]

Wang *et al.*[75] fabricated mixed matrix membranes by incorporating polyether amine grafted graphene oxide nano-fluids into a PEBAx matrix. A solvent-free hybrid nano-fluid is a new class of hybrid material, consisting of an inorganic core and an organic canopy. Graphene oxide was functionalized with some Fe_3O_4 nanoparticles, before grafted covalently with poly-ether amine forming the graphene oxide nano-fluid (P-GO-NF). The nanosheets were then incorporated into PEBAx using a drop-casting method, forming the P-GO-NF/PEBAx MMM. (Fig 3.9) CO_2 permeability increased along with an increase in filler content and was found to increase by 497% compared to the pristine PEBAx membrane, reaching 394 Barrer. However, the N_2 permeability did also increase while increasing the filler content, making the selectivity best at 20 wt% loading. The enhancement was mainly attributed to the EO-groups and secondary amines present in the poly-ether amine canopy. The best membrane performance reached 233.1 Barrer and a selectivity of 60.4 at 25 °C, 2 bar and dry state.[75]

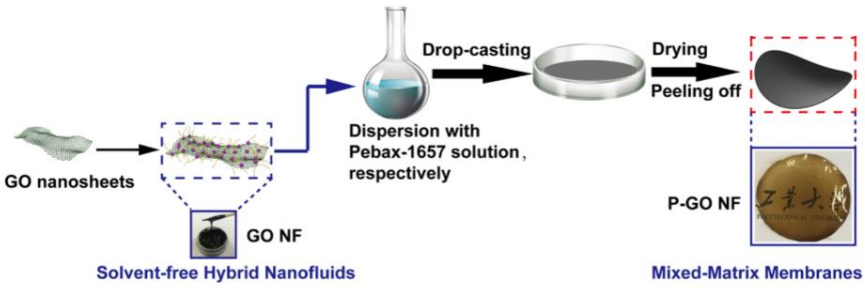

Figure 3.9: Preparation of poly-ether amine functionalized graphene oxide nano-fluid in Pebax, forming mixed matrix membranes.[75]

Huang *et al.*[76] developed MMMs by incorporating ionic liquid functionalized graphene oxide (IL-GO) into a PEBAx matrix. Graphene oxide was prepared by using the improved Hummers' method, before 3-bromopropylamine hydrobromide and 1-methylimidazole, forming the ionic liquid NH_2-IL, was added onto GO *via* an epoxide ring-opening reaction. Thereafter, membranes were generated by adding certain loadings of GO and IL-GO fillers (0.05-0.5 wt%) separately into the PEBAx matrix. (Fig 3.10) For the GO/PEBAx membranes, the best result was obtained with a filler content of 0.05 wt%, showing a CO_2 permeability of 113 Barrer and a CO_2/N_2 selectivity of 72. This corresponded to an improvement of 23% in permeability and 71% in selectivity compared to the pristine PEBAx. The enhancement could be explained by the higher CO_2 solubility in the GO/PEBAx membrane, than for the pristine PEBAX membrane. However, at higher loadings up to 0.5 wt%, both permeability and selectivity decreased due to aggregation of GO nanosheets. The same trends were to be seen for the IL-GO/PEBAx membranes, except that the best performance was obtained with filler content of 0.2 wt%. The hydrogen bonding interactions between the ionic liquid and the amide moieties in PEBAx provided a homogeneous and uniform dispersion of IL-GO, causing the membrane to possess a higher CO_2 sorption capability. Improvements in both CO_2 permeability and CO_2/N_2 selectivity was observed, showing 143 Barrer and 80, respectively.[76]

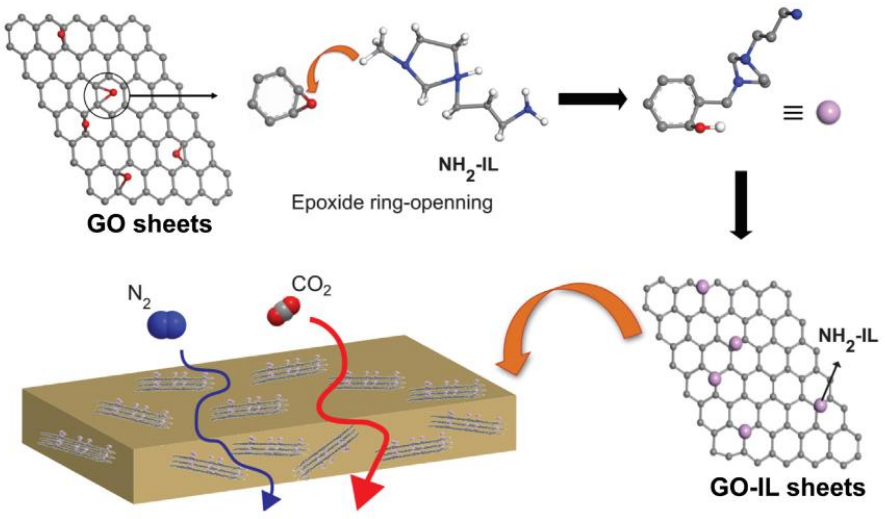

Figure 3.10: Schematic illustration of the gas transport through the IL-GO-based membrane.[76]

Yang *et al.*[77] prepared mixed matrix membranes conducted by incorporating ZIF-8 coated graphene oxide into PEBAx. ZIF-8-GO was synthesized by pre-Zn(II)-doping the graphene oxide suspension, before adding 1-methylimidazole and zinc nitrate hexahydrate using an

ultrasound-assisted treatment in an *in-situ* growth method. Following, the ZIF-8-GO fillers were dispersed into the PEBAx matrix, fabricated by solution casting. The rigid ZIF-8 layer acted like an armour suit and stretched and unfolded the graphene oxide, efficiently. (Fig 3.11) The GO sheets intercepted the general diffusion pathways, resulting in compelling the gas molecules to pass by GO barriers *via* interfacial diffusion. Moreover, the abundant oxy groups on the GO surface enhanced the CO_2/N_2 selectivity. The addition of ZIF-8 on the other hand, efficiently diminished the mass transfer resistance, much more than the resistance caused by only GO barriers in the MMM, promoting permeability and selectivity. Along with an increase in filler content, there was an increase in CO_2 permeation. However, the positive effects gradually disappeared when the filler content was higher than 20 wt%. This trend was also observed for the selectivity. The best performing MMM reached a permeability of 136.2 Barrer and a CO_2/N_2 selectivity of 77.9, enhanced by 66% and 60% compared to pristine PEBAx samples, respectively.[77]

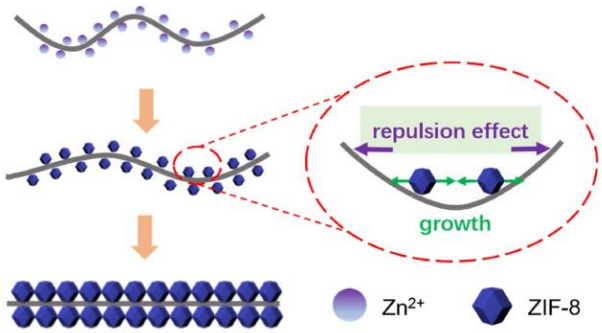

Figure 3.11: Stretching mechanism for the ZIF-8-GO armour suit synthesis process.[77]

Dong *et al.*[78] fabricated MMMs by incorporating ZIF-8-GO into a PEBAx matrix. Graphene oxide was synthesized using the modified Hummers' method, before adding zinc nitrate hexahydrate and 2-methylimidazole in a two-step ultrasound process. (Fig 3.12) ZIF-8-GO/PEBAx mixed matrix membranes with different filler loadings were then prepared by solvent evaporation. Since the graphene oxide nanosheets inherent high-aspect ratio, they offered increased length of the tortuous pathway, offering a selective barrier for the smallest molecules with less resistance, resulting in an enhanced diffusivity selectivity. Also, the additional porous ZIF-8 was expected to optimize a higher fractional free volume, consequently increasing the gas permeability of the membrane. ZIF-8-GO did also exhibit good compatibility with the PEBAx matrix, making the nanofillers well dispersed. As the ZIF-8-GO filler content

increased, the transport properties were affected, resulting in an increase of the CO_2 permeability. The same trend was also observed for the CO_2/N_2 selectivity, reaching the maximum at 6 wt%. The decrease in selectivity at higher filler contents than this was probably due to cracks and interfacial holes between the nanofillers and the matrix. Therefore, the best performance was obtained using 6 wt% filler loading, achieving a CO_2 permeability of 249 Barrer and a CO_2/N_2 selectivity of 47.6.[78]

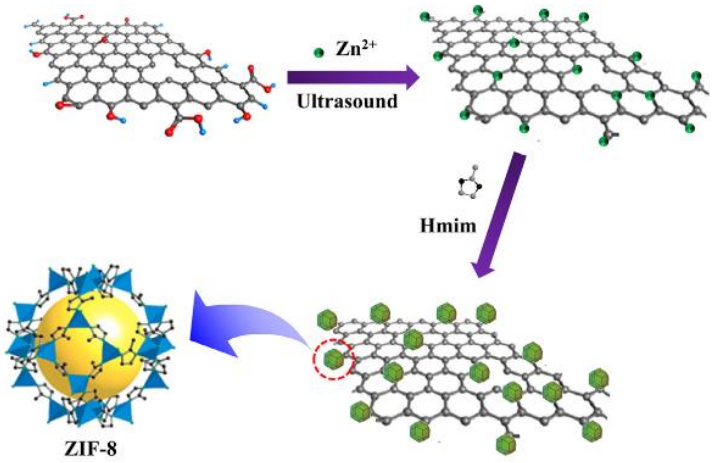

Figure 3.12: Preparation of ZIF-8-GO.[78]

Huang *et al.*[79] developed an environmentally friendly method to fabricate N-doped few-layered graphene (N-FLG) incorporated in a PEBAx matrix. (Fig 3.13) Few layered graphene was synthesized by applying high pressure (200 MPa) to deionized water and graphite, causing a shearing effect that dispersed graphene. Hexamethylenetetramine was utilized as a nitrogen precursor in the N-doping, before the N-FLG was loaded into the PEBAx matrix in 0, 0.5, 2, 3, 4, and 5 wt%. Molecular simulations were applied to predict the behaviour of interactions between the membrane and gas molecules, and to analyse the effects of the N-doping. Results showed that the addition of N-FLG improved the capture performance due to the nanofiller's affinity for CO_2 molecules. Both permeability and selectivity gradually increased with an increase in filler content at low N-doping, whilst decreasing when the loading got higher than 4 wt%, mainly because of agglomeration of the nanosheets. The best performance reached a CO_2 permeability and CO_2/N_2 selectivity of 239.8 Barrer and 95.5, respectively.[79]

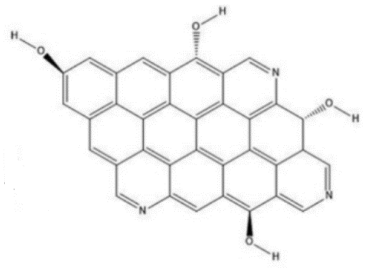

Figure 3.13: Schematic structure of N-doped graphene oxide.[79]

3.2.2 Performance of PEBAx-based Membranes at Humidified State

Zhang *et al*.[80] synthesized aminosilane-functionalized graphene oxide nanosheets as fillers for PEBAx matrix. Graphene oxide was prepared by using the Hummers' method, before 3-aminopropyltriethoxysilane (APTS) was covalently grafted to the oxygen-containing functional groups on GO using sonication. (Fig 3.14) The nanocomposites were incorporated into PEBAx, forming the complete APTS-GO/PEBAx membrane. Aminosilane operated as an interface moderator and a CO_2 carrier, resulting in the amino groups constructing a facilitated transport pathway along the interface, effectively promoting the permeability of CO_2. Compared with neat GO, APTS-GO showed improved interfacial compatibility with the polymer matrix, forming a uniform distribution. The introduction of CO_2-philic amino groups did also enhance the solubility and selectivity of CO_2, resulting in the membrane exhibiting the highest performance in humidified state at 35 °C and 2 bar, with CO_2 permeation of 934 Barrer, and $CO_2/N_2(CH_4)$ selectivity of 71.1(40.9).

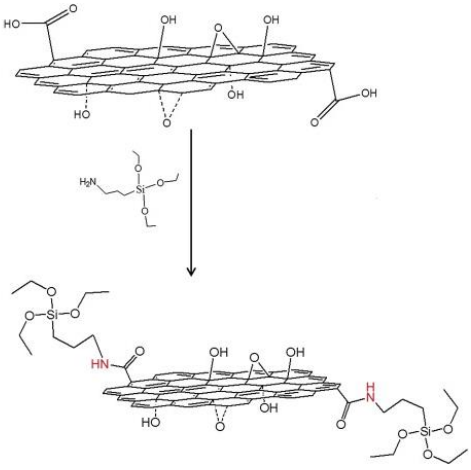

Figure 3.14: Schematic representation of introducing aminosilane to graphene oxide, obtaining the APTS-GO nanocomposites.[80]

Zhu *et al.*[81] prepared mixed-matrix membranes using PEBAx polymer incorporated by iron oxide (Fe_3O_4) functionalized graphene oxide, designed Fe_3O_4-GO/PEBAx. Graphene oxide was synthesized by using the modified Hummers' method, before Fe_3O_4 was added by a solvent-assisted method. Pure PEBAx was then loaded with fillers, followed by controlling the magnetic field direction arranging the Fe_3O_4-GO sheets horizontally or vertically. (Fig 3.15) Results showed that magnetic alignment of Fe_3O_4-GO/PEBAx presented better gas separation performance than that of a random arranged alignment. The Fe_3O_4-GO offered numerous advantages. Firstly, the induced alignment allowed for a shorter transfer pathway for the gas molecules, increasing the permeability of CO_2. Secondly, the presence of Fe_3O_4 and the hydroxyl groups in GO caused strong binding force for water, improving the CO_2 solubility selectivity. Thirdly, the interactions between the magnetic alignment of GO composites and the polymer matrix priduced a reduction in the interface defects. The effect of the nanosheets was best at a humidified state and showed best performance with a loading of 3 wt% for both horizontally and vertically arranged Fe_3O_4-GO/PEBAx. The vertical GO/PEBAx possessed the highest permeability with 538.65 Barrer and a selectivity for $CO_2/N_2(CH_4)$ of 75.11(46.21).[81]

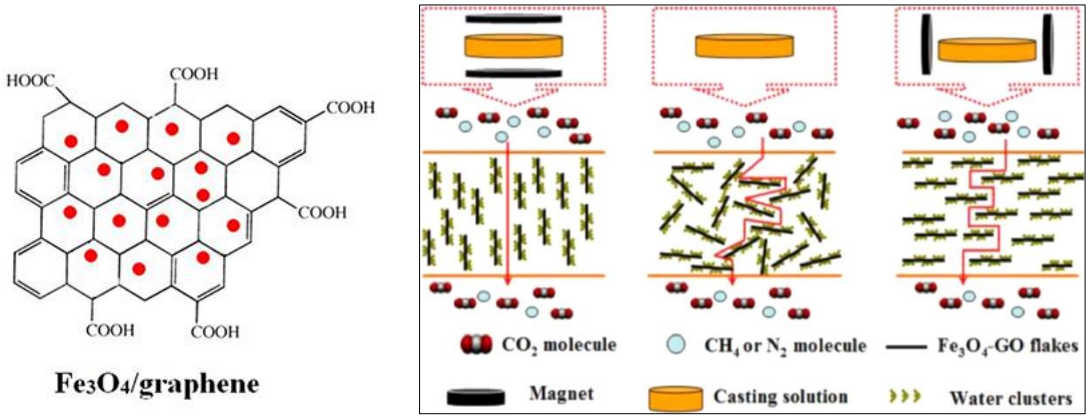

Figure 3.15: Molecular structure of Fe_3O_4-GO and different alignments of the nanosheets in the polymer matrix.[81]

Li *et al.*[33] prepared multi-permselective (MP) mixed matrix membranes by incorporating polyethylene glycol monomethyl ether (PEG, EO groups) any poly-ethylenimine (PEI, amine carriers) functionalized GO nanosheets into a PEBAx matrix. (Fig 3.16) Graphene oxide was synthesized by using the modified Hummers' method, followed by functionalizing it with PEG and PEI through repetitious sonication runs, before incorporating the PEG-PEI-GO into PEBAx by a solution-casting method. The PEG-PEI-GO had a multitude of functions in enhancing the

membrane performance. Firstly, the high-aspect ratio nanosheets increased the length of the tortuous pathway for the gas molecules and generated a rigidified interface between the polymer matrix and the fillers, enhancing the diffusivity selectivity. Secondly, the EO-consisting PEG groups had good affinity for CO_2, resulting in an enhancement for the solubility selectivity. Thirdly, the amine-consisting PEI groups reacted reversibly with CO_2, enhancing the reactivity selectivity. Thereupon, the prepared MP-MMMs exhibited excellent CO_2 permeability and CO_2 selectivity, attaining the optimal gas separation performance with 10 wt% doped PEG-PEI-GO nanosheets. The CO_2 permeability reached 1330 Barrer, and a $CO_2/N_2(CH_4)$ selectivity of 120 and 45, respectively, surpassing the Robeson upper bound.[33]

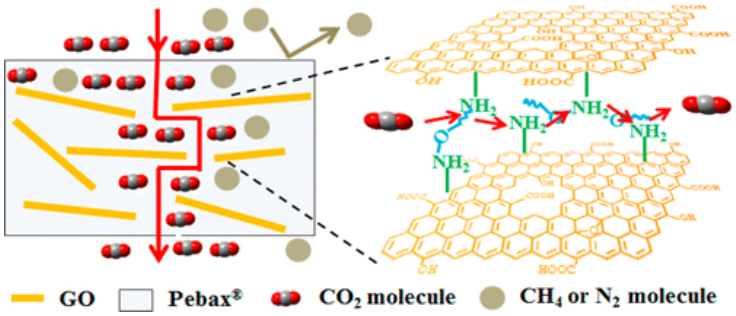

Figure 3.16: Schematic representation of the gas transport mechanism for the PEG-PEI-GO/PEBAx mixed matrix membrane.[33]

3.2.3 Compilation of Performances

Other studies have also tested PEBAx matrices in mixed matrix membranes incorporated by different nanofillers, using metal organic frameworks such as UiO-66[82] or MIL-53(Al),[83] zeolitic imidazolate frameworks (ZIF-8),[84] and tested aminated carbon nanotubes (NH_2-CNTs)[85] as well as CNTs coated with *N*-isopropylacry-lamide hydrogel (NIPAM-CNTs).[80] These membranes showed good CO_2 permeability under humidified conditions, but relatively poor CO_2/N_2 selectivity, not able to reach higher than 35. For the dry state, selectivity seemed to be better, but the permeability did not get higher than 361 Barrer. Table 3.2 presents the performances of these membranes along with the graphene-based membranes. Membranes incorporated by the graphene-based nanofillers seemed to achieve much better CO_2/N_2 selectivity and was clearly better when exposed to humidified conditions. The PEG-PEI-GO/PEBAx showed best performance, gaining a permeability of 1330 Barrer and a selectivity of 120.

Table 3.2: Comparison of CO_2 separation performance between PEBAx-based mixed matrix membranes.

Filler content	Polymer	wt% loading (best MMM performance)	Test conditions	P_{CO2} (Barrer)	CO_2/N_2 selectivity
UiO-66-NH_2[82]	PEBAx	50	Pure gas, 25 °C, 2 bar, dry state	338*	57
NH_2-MIL-53(Al)[83]	PEBAx	10	Pure gas, 35 °C, 10 bar, dry state	149	55.5
ZIF-8[84]	PEBAx	35	Pure gas, 25 °C, 2 bar, humidified state	1287	32.3
NH_2-CNT[85]	PEBAx	33	Pure gas, 35 °C, 7 bar, dry state	361	52
NIPAM-CNT[86]	PEBAx	5	Pure gas, 25 °C, 2 bar, humidified state	567	35
Im-GO[72]	PEBAx	0.8	Pure gas, 25 °C, 4 bar, dry state	64	90.3
oHAB-GO[73]	PEBAx	10-2	Mixed gas, 35 °C, 1 bar, dry state	696	51.2
A-prGO[74]	PEBAx	0.1	Pure gas, 25 °C, 4 bar, dry state	47.5	105.56
P-GO-NF[75]	PEBAx	20	Mixed gas, 25 °C, 2 bar, dry state	233.1	60.4
IL-GO[76]	PEBAx	0.2	Pure gas, 25 °C, 4 bar, dry state	143	80
ZIF-8-GO[77]	PEBAx	20	Pure gas, 25 °C, 3 bar, dry state	136.2	77.9
ZIF-8-GO[78]	PEBAx	6	Pure gas, 25 °C, 1 bar, dry state	249	47.6
N-FLG[79]	PEBAx	4	Pure gas, 25 °C, 1 bar, dry state	239.8	95.5
APTS-GO[80]	PEBAx	0.9	Mixed gas, 35 °C, 2 bar, humidified state	934	71.1
Fe_3O_4-GO[81]	PEBAx	3	Mixed gas, 25 °C, 2 bar, humidified state	538.65	75.11
PEG-PEI-GO[33]	PEBAx	10	Mixed gas, 30 °C, 2 bar, humidified state	1330	120

* Permeability unit = GPU

3.3 SPEEK-based MMMs

Sulfonated poly(ether ether ketone) (SPEEK) is a promising polymer due to its low costs, and excellent thermal and chemical stability.[87] The hydrocarbon backbones are less hydrophobic, while the sulfonic acid functional groups are less acidic and polar, resulting in a completely dispersion of water molecules once introduced into the polymer. SPEEK does therefore often undergo an aqueous swelling, providing humidified conditions, and proceeding a minimized transport resistance and increased permeability for certain molecules. (Fig 3.17)

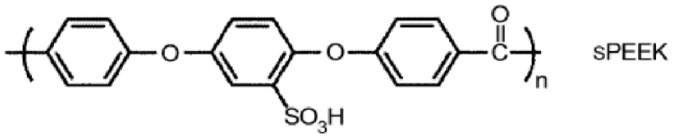

Figure 3.17: The structure of the polymeric material SPEEK.[87]

3.3.1 Performance of SPEEK-based Membranes

Xin *et al.*[88] fabricated a SPEEK-based mixed matrix membrane loaded with CO_2-philic sulfonated polymer brush functionalized graphene oxide (S-GO) nanosheets. (Fig 3.18) Exfoliated GO was obtained using the Hummers' method, followed by preparing S-GO via a non-crosslinked precipitation polymerization method, before loaded into a SPEEK matrix to fabricate the MMM. Results showed that the sulfonic acid groups in both S-GO and the SPEEK-matrix built uninterrupted transport pathways for CO_2 molecules, enhancing the CO_2 diffusivity selectivity. As the filler content of the S-GO in the MMM increased, the CO_2 permeability and the CO_2/N_2 selectivity was also improved. The best result was achieved by a loading of 8 wt% in humidified state at 25 °C and 1 bar pressure, showing CO_2 permeability of 1327 Barrer and $CO_2/N_2(CH_4)$ selectivity of 86.4(72.2), surpassing the Robeson upper bound (2008).[88]

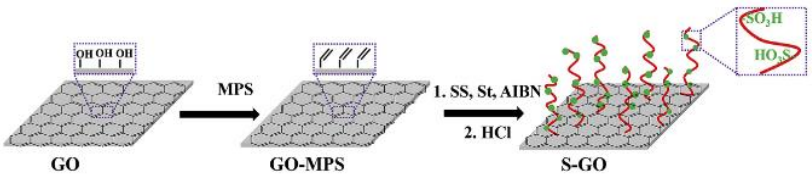

Figure 3.18: The synthesis process for obtaining sulfonated polymer brush functionalized graphene oxide (S-GO).[88]

Another MMM fabricated by Xin *et al.*[89] was conducted by incorporating amino acid functionalized graphene oxide nanosheets into a SPEEK polymer matrix. GO was prepared by using the Hummers' method, before the nanosheets were functionalized with amino acids through a facile two-step method using dopamine (DA) and cysteine (Cys), designing DA-Cys-GO nanocomposites that were introduced into the SPEEK matrix. (Fig 3.19) GO nanosheets increased more tortuous pathways for larger molecules, enhancing the diffusivity selectivity, whilst the addition of amino acids, containing carboxylic acid and primary amine groups,

enhanced the solubility selectivity and reactivity selectivity, offering CO_2 molecules to be transported faster. SPEEK polymers inherent poor gas permeability in dry state and were therefore fully humidified prior the gas permeation tests. The swelling of the membranes was also beneficial for the gas transport, due to increased intermolecular distance between the polymer chains. Both CO_2 permeability and CO_2/N_2 selectivity increased as there was an increase in the filler content, gaining the best performance at a loading of 8 wt%. Results showed that the CO_2 permeability reached 1247 Barrer and the CO_2/N_2 selectivity reached 115, significantly surpassing the Robeson upper bound.[89]

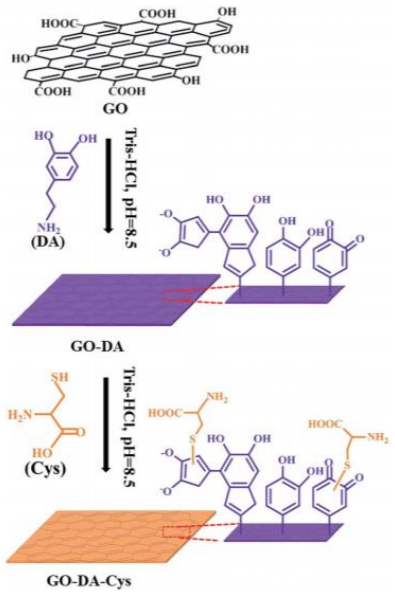

Figure 3.19: The grafting mechanism for dopamine (DA) and cysteine (Cys) on graphene oxide nanosheets.[89]

3.3.2 Compilation of Performances

SPEEK matrixes has shown excellent CO_2 permeability when being swelled up with water, and gained almost 2500 Barrer for a PEI-functionalized octahedral metal organic framework MIL-101(Cr) nanofiller.[90] Other high performance SPEEK-based membranes have been incorporated with sulfonated MOFs (S-MIL-101(Cr))[91] and pyridine-functionalized silica nanofillers.[92] These membranes performed much better than the graphene-based membranes regarding CO_2 permeability, but as shown in Table 3.3, the graphene-based nanofiller seemed to perform slightly better regarding the CO_2/N_2 selectivity.

Table 3.3: Comparison of CO_2 separation performance between SPEEK-based mixed matrix membranes.

Filler content	Polymer	wt% loading (best MMM performance)	Test conditions	P_{CO2} (Barrer)	CO_2/N_2 selectivity
S-MIL-101(Cr)[91]	SPEEK	40	Pure gas, 30 °C, 1 bar, humidified state	2064	53
PEI-MIL-101(Cr)[90]	SPEEK	40	Pure gas, 25 °C, 1 bar, humidified state	2490	80
Pyridine-silica[92]	SPEEK	20	Pure gas, 25 °C, 1 bar, humidified state	2000	68
S-GO[88]	SPEEK	8	Pure gas, 25 °C, 1 bar, humidified state	1327	86.4
DA-Cys-GO[89]	SPEEK	8	Pure gas, 25 °C, 1 bar, humidified state	1247.6	114.5

3.4 PSf-based MMMs

Poly-sulfones (PSfs) are polymers containing an aryl-SO_2-aryl subunit, which possess properties like mechanical and high thermal stability.[93] Due to the high costs concerning raw materials and processing, this type of polymer is often used as a support membrane. (Fig 3.20)

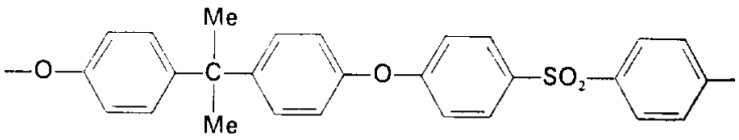

Figure 3.20: The structure of the polymeric material PSf.[93]

3.4.1 Performance of PSf-based Membranes

Shen *et al.*[94] fabricated mixed matrix membranes consisting of polyvinyl amine (PVAm) and chitosan (Cs) as the polymer matrix materials coated onto a porous poly-sulfone (PSf) support, incorporated by hyperbranched poly-ethyleneimine (HPEI) functionalized graphene oxide as the nanofillers. (Fig 3.21) HPEI was used to enhance the combability between the GO nanosheets and the polymer macromolecules, as well as to enhance the permeance and selectivity of the membrane. Cs and PVAm were used for polymer amine carriers. Graphene oxide was prepared using the modified Hummers' method, before HPEI was added, followed by synthesizing the HPEI-GO/PVAm-Cs/PSf membrane by a surface coating method.

As the filler content increased both permeation and selectivity improved compared to the neat membrane that held a CO_2 permeation of 14 GPU, N_2 permeation of 0.177 GPU, and a CO_2/N_2 selectivity of 77.6. The best performance was achieved after adding 3 wt% HPEI-GO, gaining a permeability of 31.3 GPU and a selectivity of 107. If increasing the filler content further, there was a decrease in both permeability and selectivity, mainly due to agglomeration of the nanosheets.[94]

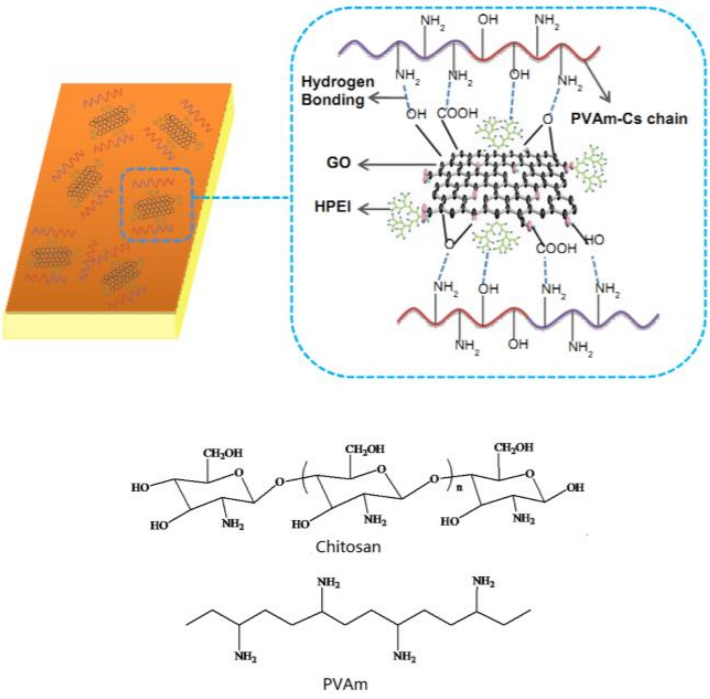

Figure 3.21: Schematic diagram of the preparation of HPEI-GO/PVAm-Cs/PSf membrane and the molecular structure of chitosan and PVAm.[94]

Another MMM using PVAm together with a PSf polymer support was fabricated by Wang *et al.*[95] who incorporated graphene oxide inserted by polyaniline (PANI) coated carbon nanotubes (PANI-CNTs-GO). (Fig 3.22) PANI and PVAm contained amino-group and helped facilitate the CO_2 transport, CNT acted as gas transport nanochannels, and GO was helping optimizing the CO_2 selective transport. Graphene oxide was synthesized using the modified Hummers' method, while PANI-CNTs were prepared by an *in-situ* polymerization method. These were mixed and centrifuged to obtain a dispersion that was added in certain amounts into PVAm, before coated on PSf. The compatibility between PVAm and the nanofillers was improved due to the electrostatic interactions and hydrogen bonding, making a uniform dispersion of the nanofillers. This facilitated the CO_2 transport as a result from the molecular sieving effect and

the effect of the reversible reactions between CO_2 and the amino groups. The best performance was attained using a membrane with filler content of 1 wt% PANI-CNTs-GO, reaching a CO_2 permeance of 170 GPU and a CO_2/N_2 selectivity of 122.4.[95]

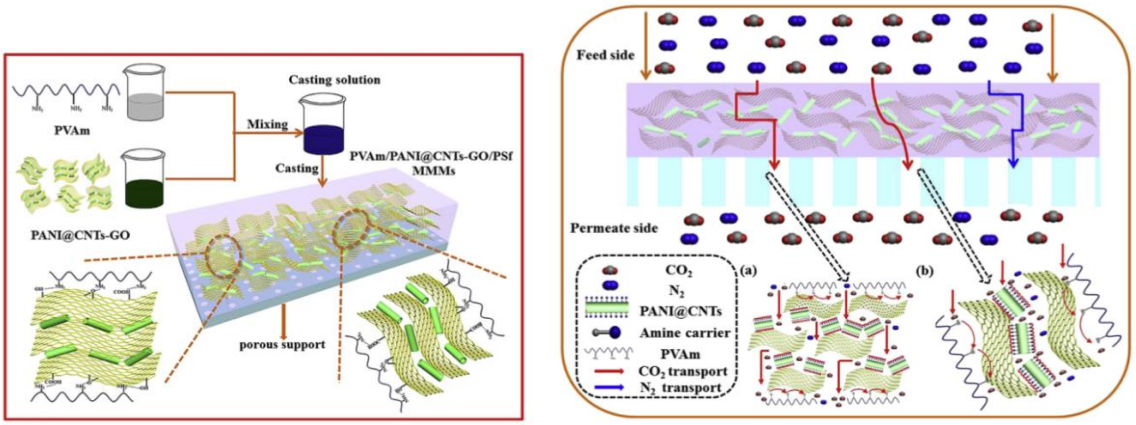

Figure 3.22: (A) Fabrication of the PANI-CNTs-GO/PVAm mixed matrix membranes, and (B) possible gas-transport routes: (a) interlayer spacing with high-speed transport; (b) interlayer spacing with tortuous transport.[95]

Dong *et al.*[96] prepared poly-sulfone (PSf) membranes coated by hyperbranched poly-ethyleneimine (HPEI), graphene oxide (GO), and trimesoyl chloride (TMC). GO was synthesized by using the modified Hummers' method, before forming an aqueous phase together with HPEI. An organic phase was containing TMC, and the membranes were constructed *via* an interfacial polymerization, adding the aqueous and organic phases onto the surface of the support membrane in a two-step process. (Fig 3.23) With an increase in the GO content, there was a concurrent increase in CO_2 permeability, additional there was an increase in the CO_2/N_2 selectivity due of a decline in the N_2 permeability. The enhancement was a consequence of the facilitated transport pathways formed from GO's high aspect ratio, and the ability to retain water molecules inside the membrane, making favourable reactions between CO_2 and amino carriers. However, higher loading than 0.33 wt% resulted in agglomeration between the nanosheets and a degradation in CO_2 permeation. The best performing sample reached a CO_2 permeance of 9.7 GPU and a CO_2/N_2 selectivity of 81.3.[96]

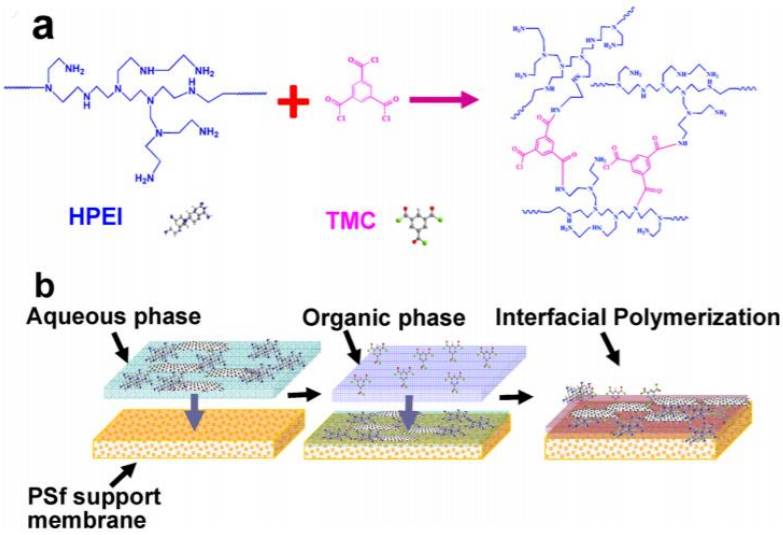

Figure 3.23: Schematic illustration of (a) the reaction between hyperbranched poly-ethylene-imine HPEI and trimesoyl chloride TMC, and (b) the preparation of the HPEI-TMC-GO/PSf membrane.[96]

Anastasiou *et al*.[97] prepared membranes consisting of ZIF-8-GO nanofillers incorporated into a poly-sulfone (PSf) matrix. (Fig 3.24) Graphene oxide was prepared using the modified Tour method, before undergoing an *in-situ* ZIF-8 growth process, in a composition of 50 wt% / 50 wt%. The ZIF-8-GO nanofillers were incorporated with a 10 wt% filler content into PSf *via* sonication and solvent evaporation. The pristine PSf membrane held a CO_2 permeability of 0.94 Barrer and a CO_2/N_2 selectivity of 0.82. However, the addition of zeolitic imidazole frameworks offered good sorption capacity, porosity, and chemical affinity, increasing the CO_2 permeability to 1.76 Barrer and decreasing the N_2 permeability to 0.36 Barrer. This led to a CO_2/N_2 selectivity of 4.89, indicating that the ZIF-8-GO nanofillers inherent much better affinity towards CO_2 than for N_2. This was due to the π-π bonds, and the hydroxyl and carboxyl functional groups on graphene oxide, making interactions with the polar gas CO_2. This led to an increase in the solubility for CO_2, whilst a decrease in the solubility for the non-polar gas N_2.[97]

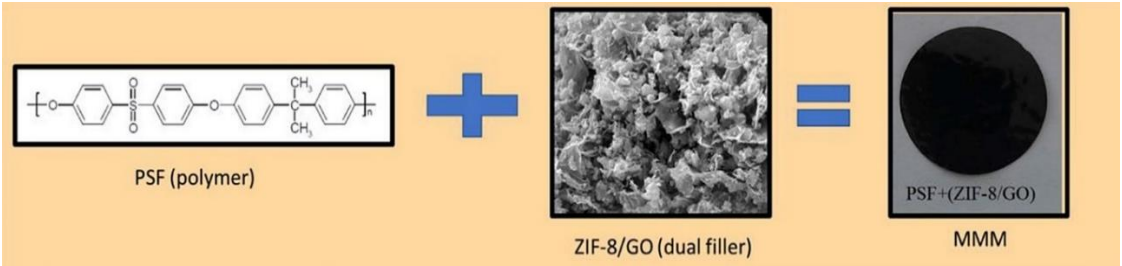

Figure 3.24: Molecular structure of PSF, an illustration of the ZIF-8-GO filler, and the complete membrane.[97]

Another PSf-based membrane containing graphene was fabricated by Sarfraz *et al.*[98] who incorporated both zeolitic imidazole frameworks (ZIF-301) and graphene oxide as nanofillers into the PSf matrix. (Fig 3.25) Results showed that membranes doped with only ZIF-301 fillers, offered improved permeability and selectivity compared to the pristine PSf membrane. Membranes doped with only GO fillers provided improved selectivity, but reduced permeability. However, membranes doped with both ZIF-301 and GO fillers showed the best performance, due to the synergistic effects between ZIF-301 and GO. The optimized membrane contained 1 wt% GO and 30 wt%, and exhibited a CO_2 permeability of 25 Barrer and a CO_2/N_2 selectivity of 63.[98]

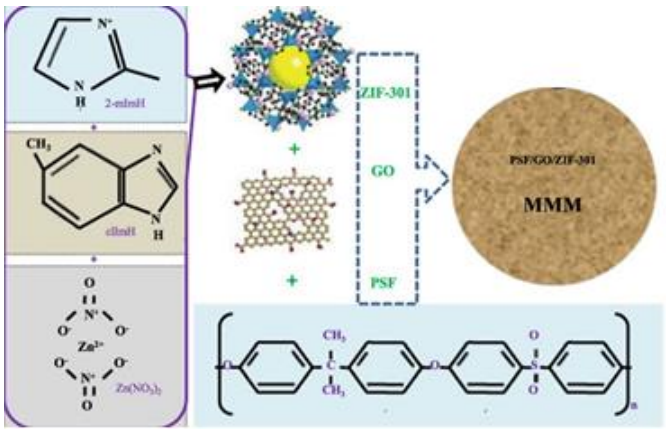

Figure 3.25: Preparation of ZIF-301-GO/PSf mixed matrix membrane.[98]

3.4.2 Compilation of Performances

PSf-based membranes have been tested with MOFs (MIL-53(Al))[99] and ZIFs (ZIF-301)[100] as well as with graphene-based materials. As shown in Table 3.4, the performances of the non-containing graphene membranes were relatively poorer than those containing graphene. For these membranes, there was an indication that it was beneficial for both CO_2 permeability and CO_2/N_2 selectivity to use PVAm together with PSf as a support, instead of using pure PSf. Additionally, humidified conditions seemed to give the best results.

Table 3.4: Comparison of CO_2 separation performance between PSf-based mixed matrix membranes.

Filler content	Polymer	wt% loading (best MMM performance)	Test conditions	P_{CO2} (Barrer)	CO_2/N_2 selectivity
MIL-53(Al)[99]	PSf	8	Pure gas, 25 °C, 3 bar, dry state	4.89	22.74
ZIF-301[100]	PSf	40	Pure gas, 25 °C, 2 bar, humidified state	21.94	32.09
HPEI-GO[94]	PVAm-Cs/PSf	3	Mixed gas, 25 °C, 1 bar, humidified state	31.3*	107
PANI-CNTs-GO[95]	PVAm/PSf	1	Pure gas, 25 °C, 1 bar, humidified state	170*	122.4
HPEI-TMC-GO[96]	PSf	0.33	Mixed gas, 30 °C, 1 bar, humidified state	9.7	81.3
ZIF-8-GO[97]	PSf	10	Pure gas, 25 °C, 4 bar, dry state	1.76	4.89
ZIF-301 GO[98]	PSf	30 1	Pure gas, 25 °C, 1 bar, dry state	25	63

* Permeability unit = GPU

3.5 PEDM- and EC-based MMMs

Other polymer matrices, incorporated by graphene-based materials, that have been tested for CO_2 separation are the advanced PEDM membrane and the ethyl cellulose (EC) membrane. (Fig 3.26) PEDM is a copolymer matrix consisting of poly(ethylene glycol) methyl ether methacrylate PEGMA, poly(N,N-dimethyl aminoethyl methacrylate) PDMAEMA and polymethyl methacrylate PMMA.[101] By mixing these polymers into a copolymer contributes to offering the matrix inherent, attractive functional units such as ethylene oxide groups and amino groups. The presence of these additional units provides enhanced solubility and reactivity selectivity for CO_2. The EC membrane on the other hand, is a derivative of cellulose, where some of the hydroxyl groups on the repeating glucose units are converted into ethyl ether groups. This membrane holds good CO_2 permeation properties, high mechanical strength, in addition to being cheap and environmentally friendly.[102]

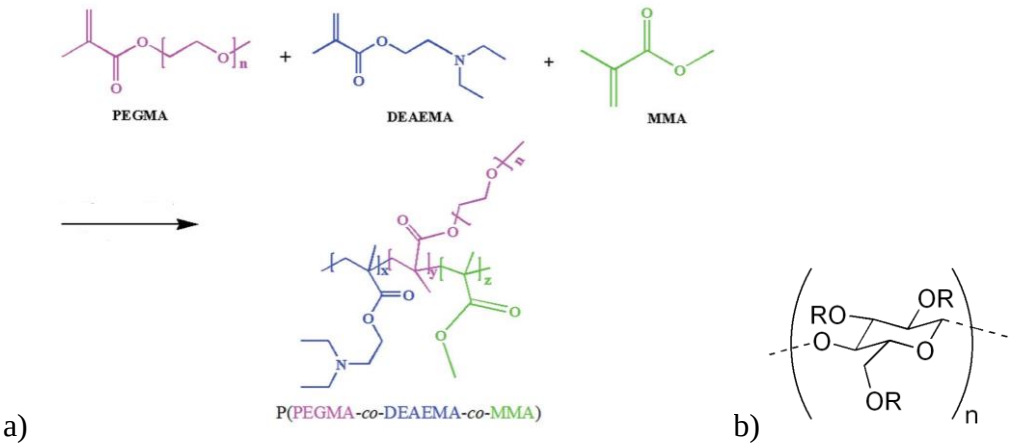

Figure 3.26: a) The synthesis and structure of PEDM,[101] and b) the structure of EC.[102]

3.5.1 Performance of PEDM- and EC-based Membranes

Chen *et al.*[101] generated ZIF-8-GO nanocomposites for incorporating a CO_2-philic comb copolymer (PEDM) to obtain ZIF-8-GO/pEDM mixed matrix membranes. Graphene oxide was synthesized using the modified Hummers' method, before zinc nitrate hexahydrate and 2-methylimidazole were added with a loading of 6 wt% and stirred for 3 h, 6 h, and 12 h, resulting in the composites designed ZIF-8-GO-3, ZIF-8-GO-6, and ZIF-8-GO-12. (Fig 3.27) The addition of inorganic fillers in the matrix disrupted the polymer chain packing, which formed more free volume and more channels for gas diffusion, providing higher permeability. CO_2 adsorption on the composites increased and then decreased along with increasing the reaction time. High CO_2 adsorption capacities were beneficial for the CO_2 adsorption of the membranes, facilitating CO_2 permeation. The high sorption of the nanofillers combined with the porosity and high free volume, resulted in a permeability of 475 Barrer for ZIF-8-GO-6. The membranes exhibited synergistic effects between the nanofillers and the comb copolymer matrix. Ethylene oxide groups and amino groups from PEDM increased the solubility selectivity and reactivity selectivity, while the ZIF-8-GO composites increased the diffusivity selectivity for CO_2/N_2, making the selectivity for CO_2/N_2 reach 58.2 and surpassing the Robeson's upper bound (2008).[101]

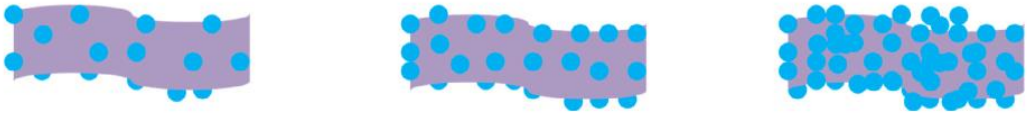

Figure 3.27: An illustration of the different densities of ZIF-8 on the GO surface with reaction time 3h, 6h, and 12 h, respectively. (The blue balls illustrate ZIF-8, while the grey sheets illustrate graphene oxide).[101]

Yang *et al.*[102] fabricated mixed matrix membranes by incorporating ZIF-8 functionalized GO into an ethyl cellulose (EC) polymer matrix. ZIF-8-GO was synthesized using a two-step ultrasonic method, involving growing ZIF-8 on the GO surface, before membranes were prepared by mixing different contents of the nanocomposites with the polymer using a cast solution process. (Fig 3.28) The functionalized ZIF-8 material offered improved CO_2 permeability due to enhanced gas transfer on the GO surface sheets and making the sheets rigid with little stacking and folding, consequently reducing the gas barrier effect. Different reaction time in fabricating the ZIF-8-GO nanosheets, did also have an impact of the permeability. As the reaction time increased, the flexible nanosheets became more and more rigid. The rigidity of the sheets caused less aggregation than pristine GO sheets, and the best performance for the membrane was obtained using a reaction time of 6 h, and a filler content of 20 wt%, achieving a CO_2 permeability of 203.3 Barrer and a CO_2/N_2 selectivity of 33.4.[102]

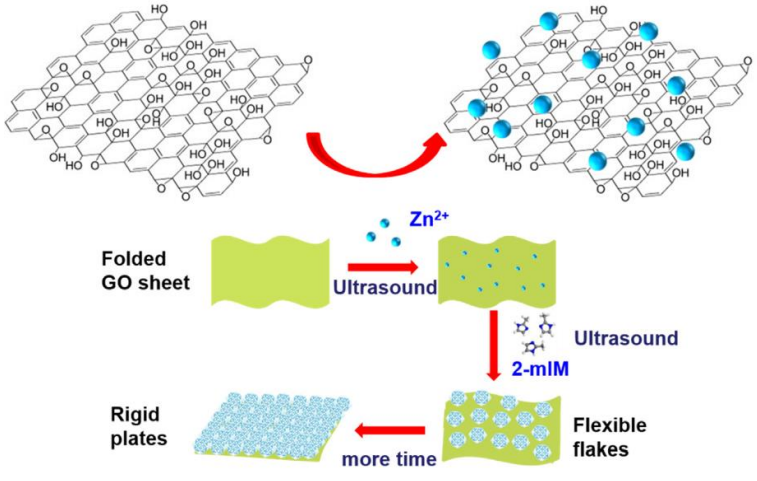

Figure 3.28: Preparation of ZIF-8-GO nanosheets.[102]

Table 3.5 presents the performances of the PEDM-based and the EC-based mixed matrix membranes. Both membranes were incorporated by ZIF-8-GO, using a reaction growth time of 6 h. The best performance was obtained using humidified conditions, mainly due to the presence of amino groups in the PEDM polymer increasing the CO_2 selectivity. EC doesn't possess any amino-groups and therefore, a humidified state would not necessarily increase the properties, indicating that PEDM might be a more favourable polymer matrix for CO_2 separation than EC.

Table 3.5: Comparison of CO_2 separation performance between the pEDM-based and the EC-based MMM.

Filler content	Polymer	wt% loading (best MMM performance)	Test conditions	P_{CO2} (Barrer)	CO_2/N_2 selectivity
ZIF-8-GO	PEDM	6	Pure gas, 25 °C, 1 bar, humidified state	475	58.2
ZIF-8-GO	EC	20	Pure gas, 25 °C, 2 bar, dry state	203.3	33.4

3.6 Summary

Table 3.6 presents a comparison of all the CO_2 separation performances between the graphene-based mixed matrix membranes.

Table 3.6: Comparison of CO_2 separation performance between graphene-based mixed matrix membranes.

Graphene	Polymer	wt% loading (best MMM performance)	Test conditions	P_{CO2} (Barrer)	CO_2/N_2 selectivity
NH_2-GO[68]	PI	3	Pure gas, 15 °C, 1 bar, dry state	12.34	38.56
UiO-NH_2-GO[69]	PI	5	Pure gas, 25 °C, 3 bar, dry state	7.28	52.0
PEG-GO[70]	PI	3	Pure gas, 30 °C, 10 bar, humidified state	370	49
Im-GO[72]	PEBAx	0.8	Pure gas, 25 °C, 4 bar, dry state	64	90.3
oHAB-GO[73]	PEBAx	10-2	Mixed gas, 35 °C, 1 bar, dry state	696	51.2
A-prGO[74]	PEBAx	0.1	Pure gas, 25 °C, 4 bar, dry state	47.5	105.56
P-GO-NF[75]	PEBAx	20	Mixed gas, 25 °C, 2 bar, dry state	233.1	60.4
IL-GO[76]	PEBAx	0.2	Pure gas, 25 °C, 4 bar, dry state	143	80
ZIF-8-GO[77]	PEBAx	20	Pure gas, 25 °C, 3 bar, dry state	136.2	77.9
ZIF-8-GO[78]	PEBAx	6	Pure gas, 25 °C, 1 bar, dry state	249	47.6

N-FLG[79]	PEBAx	4	Pure gas, 25 °C, 1 bar, dry state	239.8	95.5
APTS-GO[80]	PEBAx	0.9	Mixed gas, 35 °C, 2 bar, humidified state	934	71.1
Fe_3O_4-GO[81]	PEBAx	3	Mixed gas, 25 °C, 2 bar, humidified state	538.65	75.11
PEG-PEI-GO[33]	PEBAx	10	Mixed gas, 30 °C, 2 bar, humidified state	1330	120
S-GO[88]	SPEEK	8	Pure gas, 25 °C, 1 bar, humidified state	1327	86.4
DA-Cys-GO[89]	SPEEK	8	Pure gas, 25 °C, 1 bar, humidified state	1247.6	114.5
HPEI-GO[94]	PVAm-Cs/PSf	3	Mixed gas, 25 °C, 1 bar, humidified state	31.3*	107
PANI-CNTs-GO[95]	PVAm/PSf	1	Pure gas, 25 °C, 1 bar, humidified state	170*	122.4
HPEI-TMC-GO[96]	PSf	0.33	Mixed gas, 30 °C, 1 bar, humidified state	9.7	81.3
ZIF-8-GO[97]	PSf	10	Pure gas, 25 °C, 4 bar, dry state	1.76	4.89
ZIF-301 GO[98]	PSf	30 1	Pure gas, 25 °C, 1 bar, dry state	25	63
ZIF-8-GO	PEDM	6	Pure gas, 25 °C, 1 bar, humidified state	475	58.2
ZIF-8-GO	EC	20	Pure gas, 25 °C, 2 bar, dry state	203.3	33.4

* Permeability unit = GPU

4. Conclusion

To help deal with the impending climate crisis, incorporating carbon capture and storage (CCS) technologies in the combustion of fossil fuels is an interesting alternative as it may slow down the production of CO_2 emissions. The focal point of this thesis was therefore to analyse recent published literature on membrane separation in CCS, analysing mixed matrix membranes (MMM), in particular, consisting of polyimide (PI), poly(ether blocks amide) (PEBAx), sulfonated poly(ether ether ketone) (SPEEK), poly-sulfone (PSf), ethyl cellulose (EC), and an advanced copolymer (PEDM) as polymers, incorporated by different functionalized graphene-based materials as nanofillers. The goal was to identify which components/functional groups, decorating graphene, could effectively increase the CO_2 capturing performance.

Results showed that PEBAx and SPEEK matrices were most promising as polymers for the CO_2 capturing MMM, especially under humidified conditions. Water was then participating in reactions with CO_2, increasing the diffusion. For the components functionalizing graphene there were a multitude of units tested, involving imidazole groups, amino-groups, ionic liquids, metal organic frameworks (MOFs), zeolitic imidazole frameworks (ZIFs), ethylene oxide (EO) groups, sulfonated groups, and others. Many of these lacked the ability to possess both good permeability and selectivity, not being able to reach above the Robeson upper bound (2008). However, an interesting observation revealed that there was an increase in both permeability and selectivity along with an increase in content filler for each membrane. This trend was spotted up to a certain optimized concentration, before a decrease for both properties occurred. Degradation of properties was mainly due to agglomeration of the graphene sheets, caused by interactions effects.

Nanofillers conducted of EO- and amino functionalized graphene showed good results due to EO's good affinity towards CO_2, increasing the solubility selectivity, and amine's reversible reactions with CO_2 when water was present, contributing to an enhanced reactivity selectivity. The PEG-PEI-GO/PEBAx membrane for instance showed a CO_2 permeability of 1330 Barrer and a CO_2/N_2 selectivity of 120. Other promising nanofillers incorporated into SPEEK matrices were the CO_2-philic sulfonated polymer brush functionalized graphene oxide (S-GO) and the cysteine and dopamine functionalized graphene oxide (DA-Cys-GO), reaching permeabilities of 1327 and 1247.6 Barrer and selectivities of 86.4 and 114.5, respectively. All these membranes reached above the Robeson upper bound, emphasizing that the PEG, PEI, S, DA and Cys were functional units with good additional properties. Since this is a novel area of

research, a modified version of this thesis will be published as a review in a peer-reviewed journal.

5. Work for Future Research

Due to the corona-situation and the university shutting down, the designed experimental work was not completed. However, the promising anchoring groups and functional units attached to graphene, should be materials for future investigation regarding graphene-based mixed matrix membranes. Therefore, in this chapter, relevant organic synthetic theory will be presented along with details describing the synthetic routes and mechanisms developed for preparing the non-covalent and covalent graphene nano-ensembles.

5.1 Non-covalent Approach

This approach was originally the scope of the thesis. Esters consisting of a pyrene moiety as the anchoring group and EO-groups as the functional units were supposed to be synthesized and attached onto graphene. Different lengths of the anchoring group were supposed to be tested, before the composites were to be dispersed into a polymer matrix as nanofillers, followed by gas separation tests hopefully indicating an increase in the CO_2 capture efficiency. Only two syntheses were tested within the timeframe, involving esterification reactions utilizing pyrenyl acetic acid and pyrenyl butyric acid together with triethylene glycol. These materials were supposed to be attached onto graphene by π-π stacking. The nano-ensembles are easily obtained by mixing the organic moieties with exfoliated graphene. The unreacted organics are removed *via* filtration and washing, affording the non-covalently decorated graphene-based materials.

5.1.1 Fischer Esterification

Fischer esterification is an esterification reaction based on heating up a carboxylic acid with an alcohol in the presence of a strong acid as the catalyst. The reaction is reversible, meaning that to drive the reaction to completion, it is necessary to exploit the Le Châteliers principle. This can be done by either continuously remove the formed water from the system or by using large excess of the alcohol.[103] (Scheme 5.1)

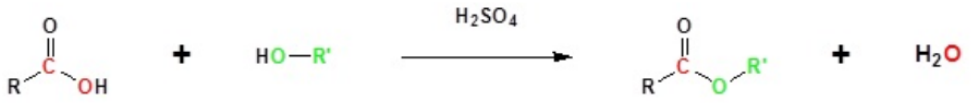

Scheme 5.1: The general synthesis of a Fischer esterification reaction.[103]

The same procedure as shown in scheme 5.1 was utilized to design reactions synthesizing 2-(2-(2-ethoxy ethoxy)ethoxy)ethyl 2-(pyren-2-yl)acetate and 2-(2-(2-ethoxy ethoxy)ethoxy)ethyl 4-(pyren-2-yl)butanoate. (Scheme 5.2, Scheme 5.3)

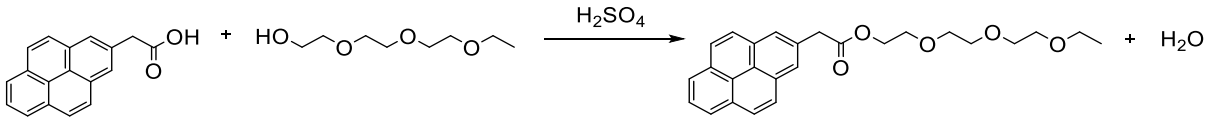

Scheme 5.2: The synthesis of 2-(2-(2-ethoxy ethoxy)ethoxy)ethyl 2-(pyren-2-yl)acetate in a Fischer esterification reaction using 2-(pyren-2-yl)acetic acid and 2-(2-(2-ethoxyethoxy)ethoxy)ethan-1-ol.

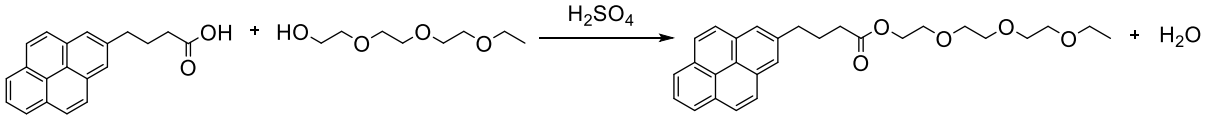

Scheme 5.3: The synthesis of 2-(2-(2-ethoxy ethoxy)ethoxy)ethyl 4-(pyren-2-yl)butanoate in a Fischer esterification reaction using 4-(pyren-2-yl)butanoic acid and 2-(2-(2-ethoxyethoxy)ethoxy)ethan-1-ol.

The mechanism for the reactions involves a protonation of the carbonyl by the acid, leading the carbonyl to be activated towards a nucleophilic attack by the alcohol. Following, there is a proton transfer, before water leaves and a deprotonation by the conjugated base forms the complete ester. (Scheme 5.4)

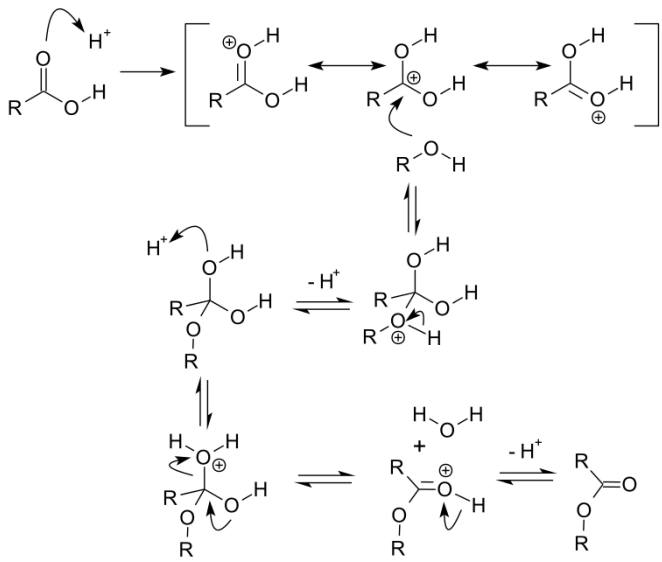

Scheme 5.4: Mechanism for the Fischer esterification reaction.

5.2 Covalent Approach

This approach was a co-student's project, where the synthesized material was supposed to be covalently attached onto graphene using the Bingel reaction. The functional unit was malonate, synthesized by a nucleophilic acyl substitution. The participation in this project allowed for a familiarization on graphene production as well as handling of this material.

5.2.1 Nucleophilic Acyl Substitution

Nucleophilic acyl substitutions describe a class of substitution reactions which involve nucleophiles and acyl compounds.[104] The reaction processes through a nucleophile, often an alcohol, amine or enolate, substituting a leaving group on the acyl derivative. The derivative is often an acid halogenate, an anhydride or an ester.[104] These types of reactions can be used to synthesize a numerous of different products. Economopoulos *et al.* synthesized antracen-9-yl methyl methyl malonate in an esterification via a nucleophilic acyl substitution of methyl-3-chloro-3-oxopropanate with anthracen-9-yl methanol.[105] (Scheme 5.5.)

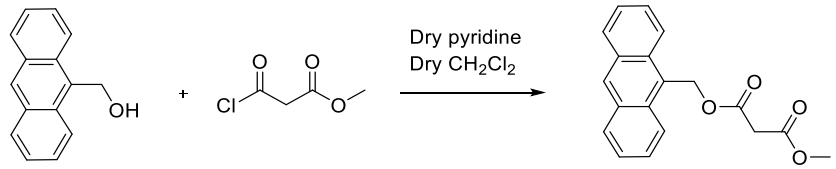

Scheme 5.5: The synthesis of antracen-9-yl methyl methyl malonate in an esterification via a nucleophilic acyl substitution of methyl 3-chloro-3-oxopropanate with anthracen-9-yl methanol.[105]

The same procedure as shown in scheme 5.4 was utilized to design a synthetic route by co-student Lucasen,[106] replacing the anthracene alcohol with 2-(2-(2-ethoxy ethoxy)ethoxy)ethane-1-ol, and methyl 3-chloro-3-oxopropanate with ethyl 3-chloro-3-oxopropanate, giving 2-(2-(2-ethoxy ethoxy)ethoxy)ethyl methyl malonate as the product. This synthesis became a standard procedure in the lab. (Scheme 5.6)

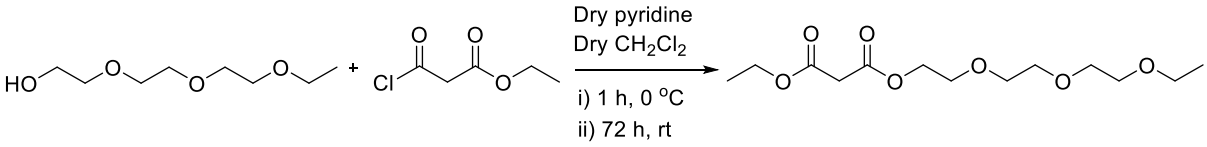

Scheme 5.6: The synthesis of 2-(2-(2-ethoxy ethoxy)ethoxy)ethyl ethyl malonate in an esterification via a nucleophilic acyl substitution of 2-(2-(2-ethoxy ethoxy)ethoxy)ethane-1-ol with ethyl 3-chloro-3-oxopropanate.

The mechanism for the reaction relies on malonyl chloride and glycol reacting in an addition mechanism making a tetrahedral intermediate. Chloride is then eliminated, before the chloride ion is deprotonating the alcohol group creating the malonate product. (Scheme 5.7)

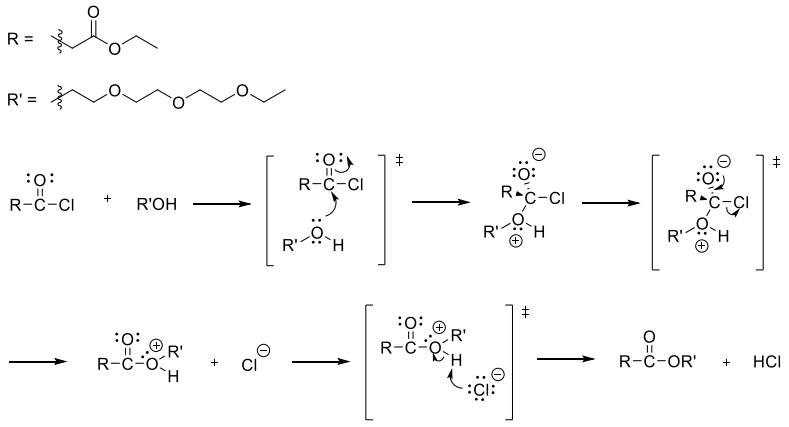

Scheme 5.7: Mechanism for the preparation of malonate.

5.3 Further Recommendation

As a further recommendation, these materials should be attached onto graphene and dispersed into a polymer matrix to complete the mixed matrix membranes. In order to obtain a thorough research, more derivatives should be included, exploring various anchoring lengths, moieties and functional units. Incorporating amine groups could also be beneficial due to the good potential in increasing the CO_2 selectivity. Another recommendation is to test the membranes from the literature study that were tested in dry conditions, in humidified conditions, as water seemed to have a great impact on the performance. Other promising nanofillers that also should be tested in PEBAx or SPEEK polymers under humidified conditions, are the PANI-CNTs-GO and HPEI-GO, because of the good potential for CO_2/N_2 selectivity, reaching over 100.

6. Experimental

6.1 General Methods

All synthesis and analyses were done at the Department of Chemistry, faculty of Natural Science, Norwegian University of Science and Technology, Trondheim, Norway.

6.1.1 Chemicals and Solvents

All chemicals and reagents used for the synthesis and analyses were bought from SigmaAldrich, Oslo, Norway.

6.1.2 Spectroscopic Analyses

Nuclear magnetic resonance spectroscopy (NMR)

Bruker 400 MHz Avance III HD system equipped with a 5 mm SmartProbe z-gradient probe and SampleCase.

6.2 Synthesis of Functionalization Groups

6.2.1 Synthesis of 2-(2-(2-Ethoxy Ethoxy)Ethoxy)Ethyl 2-(Pyren-2-yl)Acetate

Pyrenyl acetic acid (0.1216 g, $4.67 \cdot 10^{-4}$ mol) was dissolved in an excess of tri(ethylene glycol) monoethyl ether (4 mL) with 2 drops of sulfuric acid (H_2SO_4). The mixture was heated up to ~ 120 °C and the reaction was monitored by TLC. After t = 3 h the reaction was terminated by adding brine. The organic and aqueous layers were separated and washed/extracted (3 x 50 mL of ethyl acetate/water). The organic layer was dried over anhydrous sodium sulphate, filtrated, and evaporated under reduced pressure. Unfortunately, ^{1}H-NMR did not reveal any product.

6.2.2 Synthesis of 2-(2-(2-Ethoxy Ethoxy)Ethoxy)Ethyl 4-(Pyren-2-yl)Butanoate

Pyrenyl butanoic acid (0.1211 g, $4.20 \cdot 10^{-4}$ mol) and tri(ethylene glycol) monoethyl ether (0.074 mL, $4.18 \cdot 10^{-4}$ mol) were solved in toluene (9 mL) before adding a tip of spatula *p*-toluene sulfonic acid as the catalyst. The mixture was placed in a Dean-Stark apparatus and heated up to ~ 120 °C under reflux for 24 h. The reaction was terminated by adding a NaOH-solution. THF was added to facilitate solubility of the precipitate, before separating the organic layers and washing/extracting it (3 x 50 mL of ethyl acetate/water). The organic layer was dried over anhydrous sodium sulphate, filtrated, and evaporated under reduced pressure. This gave a polluted crude with a yield of 71.5%. Both TLC and ^{1}H-NMR indicated presence of product, but time constraints did not allow to complete the work up. ^{1}H-NMR (400 MHz, $CDCl_3$) δ: 8.29-8.26 (m, 1.6H), 8.14-8.06 (m, 5.1H), 7.99-7.93 (m, 6.8H), 7.84-7.82 (m, 1.6H), 4.23 (t, 2H), 3.65 (t, 2H), 3.61-3.48 (m, 8H), 3.44 (q, 2H), 3.38-3.34 (m, 2H), 2.46-2.44 (m), 2.21-2.18 (m), 1.15 (t, 3H).

6.2.3 Synthesis of 2-(2-(2-Ethoxy Ethoxy)Ethoxy)Ethyl Ethyl Malonate

This synthesis was synthesized according to the lab procedure, ref. Sigmund NMR Dry CH_2Cl_2 (50 mL), dry pyridine (1 mL, excess) and tri(ethylene glycol) monoethyl ether (1,75 mL) was mixed and cooled to 0 degrees. Ethyl malonyl chloride (1,28 mL) was added slowly, stirred for 1 hour at 0 degrees, and then stirred in inert atmosphere in room temperature for 72 h. The reaction was terminated by adding brine, followed by separating the organic and aqueous layers and washing/extracting them furtherly. At last the organic layer was dried over anhydrous magnesium sulphate, filtrated and evaporated under reduced pressure. This gave a 94,8% yield of malonate (2,77 g, 9,48 mmol). ^{1}H-NMR (400 MHz, $CDCl_3$) δ: 4,319-4,295 (t, 2H), 4,233-4,180 (q, 3H), 3,731-3,707 (t, 2H), 3,661-3,580 (m, 8H), 3,555-3,502 (q, 3H), 3,406 (s, 2H), 1,301-1,265 (t, 3H), 1,229-1,194 (t, 3H).

6.3 Exfoliating Graphene

Graphene was exfoliated by sonicating graphite (500 mg) in 1-methyl-2-pyrrolidone (30 mL) at 90% (60 Watt) in a Bandelin SONOPULS HD2070 70W sonicator for 30 min, while the vial was placed in an icebath (1 L). The product was centrifuged (4000 rpm, 7 min) to separate the

exfoliated supernatant from residual graphite. Finally, the supernatant was re-dispersed in 1,2-dichlorobenzene (o-DCB) through filtrating using an Omnipore 0.45 µm PTFE membrane, and sonicating the filtercake in ~ 10 mL of d-DCB to yield the exfoliated graphene starting material.

Bibliography

1. Leung, D. Y. C.; Caramanna, G.; Maroto-Valer, M. M., An overview of current status of carbon dioxide capture and storage technologies. *Renewable and Sustainable Energy Reviews* **2014,** *39*, 426-443.
2. Lackner, K., Comparative Impacts of Fossil Fuels and Alternative Energy Sources. *Carbon Capture Sequestration and Storage; Issues in Environmental Science and Technology* **2010,** *29*.
3. D'Alessandro, D. M.; Smit, B.; Long, J. R., Carbon dioxide capture: Prospects for new materials. *Angewandte Chemie - International Edition* **2010,** *49* (35), 6058-6082.
4. Lee, S.-Y.; Park, S.-J., A review on solid adsorbents for carbon dioxide capture. *Journal of Industrial and Engineering Chemistry* **2015,** *23*, 1-11.
5. Jacobson, M. Z., Review of solutions to global warming, air pollution, and energy security. *Energy and Environmental Science* **2009,** *2* (2), 148-173.
6. Yang, H.; Xu, Z.; Fan, M.; Gupta, R.; Slimane, R. B.; Bland, A. E.; Wright, I., Progress in carbon dioxide separation and capture: A review. *Journal of Environmental Sciences* **2008,** *20* (1), 14-27.
7. Mondal, M.; Balsora, H.; Varshney, P., Progress and trends in CO2 capture/separation technologies: A review. *Energy* **2012,** *46*, 431–441.
8. Brunetti, A.; Scura, F.; Barbieri, G.; Drioli, E., Membrane technologies for CO2 separation. *Journal of Membrane Science* **2010,** *359* (1-2), 115-125.
9. Merkel, T. C.; Lin, H.; Wei, X.; Baker, R., Power plant post-combustion carbon dioxide capture: An opportunity for membranes. *Journal of Membrane Science* **2010,** *359* (1-2), 126-139.
10. Verma, C.; Ebenso, E. E., Ionic liquid-mediated functionalization of graphene-based materials for versatile applications: a review. *Graphene Technology* **2019,** *4* (1), 1-15.
11. Andirova, D.; Cogswell, C. F.; Lei, Y.; Choi, S., Effect of the structural constituents of metal organic frameworks on carbon dioxide capture. *Microporous and Mesoporous Materials* **2016,** *219*, 276-305.
12. Rodenas, T.; Luz, I.; Prieto, G.; Seoane, B.; Miro, H.; Corma, A.; Kapteijn, F.; Llabrés i Xamena, F. X.; Gascon, J., Metal–organic framework nanosheets in polymer composite materials for gas separation. *Nature Materials* **2015,** *14* (1), 48-55.

13. Eddaoudi, M.; Sava, D. F.; Eubank, J. F.; Adil, K.; Guillerm, V., Zeolite-like metal–organic frameworks (ZMOFs): design, synthesis, and properties. *Chemical Society Reviews* **2015,** *44* (1), 228-249.

14. Oueiny, C.; Berlioz, S.; Perrin, F., Carbon nanotube–polyaniline composites Review Article. *Progress in Polymer Science* **2013,** *39*.

15. Ebadi Amooghin, A.; Mashhadikhan, S.; Sanaeepur, H.; Moghadassi, A.; Matsuura, T.; Ramakrishna, S., Substantial breakthroughs on function-led design of advanced materials used in mixed matrix membranes (MMMs): A new horizon for efficient CO2 separation. *Progress in Materials Science* **2019,** *102*, 222-295.

16. Bazylewski, P.; Fanchini, G., 1.13 - Graphene: Properties and Applications. In *Comprehensive Nanoscience and Nanotechnology (Second Edition)*, Andrews, D. L.; Lipson, R. H.; Nann, T., Eds. Academic Press: Oxford, **2019,** 287-304.

17. Karfa, P.; De, S.; Majhi, K. C.; Madhuri, R.; Sharma, P. K., 2.07 - Functionalization of Carbon Nanostructures. In *Comprehensive Nanoscience and Nanotechnology (Second Edition)*, Andrews, D. L.; Lipson, R. H.; Nann, T., Eds. Academic Press: Oxford, **2019,** 123-144.

18. Park, H. B.; Kamcev, J.; Robeson, L. M.; Elimelech, M.; Freeman, B. D., Maximizing the right stuff: The trade-off between membrane permeability and selectivity. *Science* **2017,** *356* (6343), 1138-1148.

19. Ji, G.; Zhao, M., Membrane Separation Technology in Carbon Capture. In *Recent Advances in Carbon Capture and Storage*, Intech: **2017**.

20. Stern, S. A., The "barrer" permeability unit. *Journal of Polymer Science Part A-2: Polymer Physics* **1968,** *6* (11), 1933-1934.

21. Hägg, M.-B., Gas Permeation Unit (GPU). In *Encyclopedia of Membranes*, Drioli, E.; Giorno, L., Eds. Springer Berlin Heidelberg: Berlin, Heidelberg, **2016,** 849-849.

22. Robeson, L. M., The upper bound revisited. *Journal of Membrane Science* **2008,** *320* (1), 390-400.

23. Noble, R., Perspectives on mixed matrix membranes. *Fuel and Energy Abstracts* **2011,** *378*, 393-397.

24. Goh, K.; Karahan, H. E.; Yang, E.; Bae, T. H., Graphene-based membranes for CO2/CH4 separation: Key challenges and perspectives. *Applied Sciences (Switzerland)* **2019,** *9* (14).

25. Hu, Q.; Marand, E.; Dhingra, S.; Fritsch, D.; Wen, J.; Wilkes, G., Poly(amide-imide)/TiO2 nano-composite gas separation membranes: Fabrication and characterization. *Journal of Membrane Science* **1997,** *135* (1), 65-79.

26. Vu, D. Q.; Koros, W. J.; Miller, S. J., Mixed matrix membranes using carbon molecular sieves: II. Modeling permeation behavior. *Journal of Membrane Science* **2003,** *211* (2), 335-348.

27. Ebert, K.; Fritsch, D.; Koll, J.; Tjahjawiguna, C., Influence of inorganic fillers on the compaction behaviour of porous polymer based membranes. *Journal of Membrane Science* **2004,** *233*, 71-78.

28. Dai, L.; Chang, D. W.; Baek, J.-B.; Lu, W., Carbon Nanomaterials for Advanced Energy Conversion and Storage. *Small* **2012,** *8* (8), 1130-1166.

29. Gadipelli, S.; Guo, Z. X., Graphene-based materials: Synthesis and gas sorption, storage and separation. *Progress in Materials Science* **2015,** *69*, 1-60.

30. Malekian, F.; Ghafourian, H.; Zare, K.; Sharif, A. A.; Zamani, Y., Recent progress in gas separation using functionalized graphene nanopores and nanoporous graphene oxide membranes. *European Physical Journal Plus* **2019,** *134* (5).

31. Aroon, M. A.; Ismail, A. F.; Matsuura, T.; Montazer-Rahmati, M. M., Performance studies of mixed matrix membranes for gas separation: A review. *Separation and Purification Technology* **2010,** *75* (3), 229-242.

32. Bertelle, S.; Gupta, T.; Roizard, D.; Vallières, C.; Favre, E., Study of polymer-carbon mixed matrix membranes for CO2 separation from flue gas. *Desalination* **2006,** *199* (1), 401-402.

33. Li, X.; Cheng, Y.; Zhang, H.; Wang, S.; Jiang, Z.; Guo, R.; Wu, H., Efficient CO2 Capture by Functionalized Graphene Oxide Nanosheets as Fillers To Fabricate Multi-Permselective Mixed Matrix Membranes. *ACS Applied Materials & Interfaces* **2015,** *7* (9), 5528-5537.

34. Zhang, X.; Browne, W.; Wees, B.; Feringa, B., Preparation of Graphene by Solvent Dispersion Methods and Its Functionalization through Noncovalent and Covalent Approaches. **2018,** 187-203.

35. Novoselov, K. S.; Geim, A. K.; Morozov, S. V.; Jiang, D.; Zhang, Y.; Dubonos, S. V.; Grigorieva, I. V.; Firsov, A. A., Electric Field Effect in Atomically Thin Carbon Films. *Science* **2004,** *306* (5696), 666.

36. Yi, M.; Shen, Z., A review on mechanical exfoliation for the scalable production of graphene. *Journal of Materials Chemistry A* **2015,** *3* (22), 11700-11715.

37. Berger, C.; Song, Z.; Li, T.; Li, X.; Ogbazghi, A. Y.; Feng, R.; Dai, Z.; Marchenkov, A. N.; Conrad, E. H.; First, P. N.; de Heer, W. A., Ultrathin Epitaxial Graphite: 2D Electron Gas

Properties and a Route toward Graphene-based Nanoelectronics. *The Journal of Physical Chemistry B* **2004,** *108* (52), 19912-19916.

38. Huang, H.; Chen, S.; Wee, A. T. S.; Chen, W., 1 - Epitaxial growth of graphene on silicon carbide (SiC). In *Graphene*, Skákalová, V.; Kaiser, A. B., Eds. Woodhead Publishing: **2014,** 3-26.

39. Chng, C. E.; Ambrosi, A.; Chua, C. K.; Pumera, M.; Bonanni, A., Chemically Reduced Graphene Oxide for the Assessment of Food Quality: How the Electrochemical Platform Should Be Tailored to the Application. *Chemistry – A European Journal* **2017,** *23* (8), 1930-1936.

40. Kaniyoor, A.; Baby, T. T.; Ramaprabhu, S., Graphene synthesis via hydrogen induced low temperature exfoliation of graphite oxide. *Journal of Materials Chemistry* **2010,** *20* (39), 8467-8469.

41. Pei, S.; Cheng, H.-M., The reduction of graphene oxide. *Carbon* **2012,** *50* (9), 3210-3228.

42. Coleman, J. N., Liquid Exfoliation of Defect-Free Graphene. *Accounts of Chemical Research* **2013,** *46* (1), 14-22.

43. Hernandez, Y.; Nicolosi, V.; Lotya, M.; Blighe, F. M.; Sun, Z.; De, S.; McGovern, I. T.; Holland, B.; Byrne, M.; Gun'Ko, Y. K.; Boland, J. J.; Niraj, P.; Duesberg, G.; Krishnamurthy, S.; Goodhue, R.; Hutchison, J.; Scardaci, V.; Ferrari, A. C.; Coleman, J. N., High-yield production of graphene by liquid-phase exfoliation of graphite. *Nature Nanotechnology* **2008,** *3* (9), 563-568.

44. Hadi, A.; Zahirifar, J.; Karimi-Sabet, J.; Dastbaz, A., Graphene nanosheets preparation using magnetic nanoparticle assisted liquid phase exfoliation of graphite: The coupled effect of ultrasound and wedging nanoparticles. *Ultrasonics Sonochemistry* **2018,** *44*, 204-214.

45. Yan, M., Pristine graphene: functionalization, fabrication, and nanocomposite materials. *Journal of physics : conference series* **2018,** *1143*.

46. Georgakilas, V.; Otyepka, M.; Bourlinos, A. B.; Chandra, V.; Kim, N.; Kemp, K. C.; Hobza, P.; Zboril, R.; Kim, K. S., Functionalization of Graphene: Covalent and Non-Covalent Approaches, Derivatives and Applications. *Chemical Reviews* **2012,** *112* (11), 6156-6214.

47. Wang, S.; Tian, Z.; Feng, J.; Wu, H.; Li, Y.; Liu, Y.; Li, X.; Xin, Q.; Jiang, Z., Enhanced CO2 separation properties by incorporating poly(ethylene glycol)-containing polymeric submicrospheres into polyimide membrane. *Journal of Membrane Science* **2015,** *473*, 310-317.

48. Li, Y.; Wang, S.; Wu, H.; Guo, R.; Liu, Y.; Jiang, Z.; Tian, Z.; Zhang, P.; Cao, X.; Wang, B., High-Performance Composite Membrane with Enriched CO2-philic Groups and Improved Adhesion at the Interface. *ACS applied materials & interfaces* **2014,** *6*.

49. Zhao, Y.; Ho, W. S. W., CO_2-Selective Membranes Containing Sterically Hindered Amines for CO_2/H_2 Separation *Ind. Eng. Chem. Res.* **2013**, 52, 8774-8782.

50. Loh, K. P.; Bao, Q.; Ang, P. K.; Yang, J., The chemistry of graphene. *Journal of Materials Chemistry* **2010,** *20* (12), 2277-2289.

51. Kiely, A. F.; Haddon, R. C.; Meier, M. S.; Selegue, J. P.; Brock, C. P.; Patrick, B. O.; Wang, G.-W.; Chen, Y., The First Structurally Characterized Homofullerene (Fulleroid). *Journal of the American Chemical Society* **1999,** *121* (34), 7971-7972.

52. Liu, W.; Speranza, Functionalization of Carbon Nanomaterials for Biomedical Applications. **2019,** *5*, 72.

53. Camps, X.; Hirsch, A., Efficient cyclopropanation of C60 starting from malonates. *Journal of the Chemical Society, Perkin Transactions 1* **1997,** (11), 1595-1596.

54. Economopoulos, S. P.; Rotas, G.; Miyata, Y.; Shinohara, H.; Tagmatarchis, N., Exfoliation and Chemical Modification Using Microwave Irradiation Affording Highly Functionalized Graphene. Washington D.C. :, **2010,** 7499-7507.

55. Tasis, D.; Tagmatarchis, N.; Bianco, A.; Prato, M., Chemistry of carbon nanotubes. *Chem Rev* **2006,** *106* (3), 1105-36.

56. Riley, K. E.; Pitonak, M.; Jurecka, P.; Hobza, P., *Chem. Rev.* **2010,** *110*, 5023.

57. Tarakeshwar, P.; Choi, H. S.; Kim, K. S., *Chem. Rev.* **2001,** *100*, 4145.

58. Hobza, P.; Bludský, O.; Selzle, H. L.; Schlag, E. W., *J. Chem. Phys.* **1992,** (97), 335;

59. Tarakeshwar, P.; Kim, K. S.; Kraka, E.; Cremer, D., Structure and stability of fluorine-substituted benzene-argon complexes: The decisive role of exchange-repulsion and dispersion interactions. *The Journal of Chemical Physics* **2001,** *115* (13), 6018-6029.

60. Sarkhel, S.; Rich, A.; Egli, M., Water−Nucleobase "Stacking": H−π and Lone Pair−π Interactions in the Atomic Resolution Crystal Structure of an RNA Pseudoknot. *Journal of the American Chemical Society* **2003,** *125* (30), 8998-8999.

61. Burley, S. K.; Petsko, G. A., Aromatic-aromatic interaction: a mechanism of protein structure stabilization. *Science* **1985,** *229* (4708), 23-8.

62. Dougherty, D. A., The cation-π interaction. *Accounts of chemical research* **2013,** *46* (4), 885-893.

63. Schottel, B. L.; Chifotides, H. T.; Dunbar, K. R., Anion-π interactions. *Chemical Society Reviews* **2008,** *37* (1), 68-83.

64. Bryant, R. G., Polyimides. *Ullmann's Encyclopedia of Industrial Chemistry* **2014**.

65. Wang, Z.; Wang, D.; Zhang, S.; Hu, L.; Jin, J., Interfacial Design of Mixed Matrix Membranes for Improved Gas Separation Performance. *Advanced Materials* **2016,** *28* (17), 3399-3405.

66. Gao, J.; Mao, H.; Jin, H.; Chen, C.; Feldhoff, A.; Li, Y., Functionalized ZIF-7/Pebax® 2533 mixed matrix membranes for CO2/N2 separation. *Microporous and Mesoporous Materials* **2020,** *297*, 110030.

67. Sun, H.; Wang, T.; Xu, Y.; Gao, W.; Li, P.; Niu, Q. J., Fabrication of polyimide and functionalized multi-walled carbon nanotubes mixed matrix membranes by in-situ polymerization for CO2 separation. *Separation and Purification Technology* **2017,** *177*, 327-336.

68. Ge, B.-S.; Wang, T.; Sun, H.-X.; Gao, W.; Zhao, H.-R., Preparation of mixed matrix membranes based on polyimide and aminated graphene oxide for CO2 separation. *Polymers for Advanced Technologies* **2018,** *29* (4), 1334-1343.

69. Jia, M.; Feng, Y.; Qiu, J.; Zhang, X.-F.; Yao, J., Amine-functionalized MOFs@GO as filler in mixed matrix membrane for selective CO2 separation. *Separation and Purification Technology* **2019,** *213*, 63-69.

70. Wu, L.-g.; Yang, C.-h.; Wang, T.; Zhang, X.-y., Enhanced the performance of graphene oxide/polyimide hybrid membrane for CO2 separation by surface modification of graphene oxide using polyethylene glycol. *Applied Surface Science* **2018,** *440*, 1063-1072.

71. Eustache, R. P., Poly(Ether-*b*-Amide) Thermoplastic Elastomers: Structure, Properties, and Applications. In *Handbook of Condensation Thermoplastic Elastomers*, (Ed)., S. F., Ed. **2006**.

72. Dai, Y.; Ruan, X.; Yan, Z.; Yang, K.; Yu, M.; Li, H.; Zhao, W.; He, G., Imidazole functionalized graphene oxide/PEBAX mixed matrix membranes for efficient CO2 capture. *Separation and Purification Technology* **2016,** *166*, 171-180.

73. Cong, S.; Li, H.; Shen, X.; Wang, J.; Zhu, J.; Liu, J.; Zhang, Y.; Van der Bruggen, B., Construction of graphene oxide based mixed matrix membranes with CO2-philic sieving gas-transport channels through strong π–π interactions. *Journal of Materials Chemistry A* **2018,** *6* (37), 17854-17860.

74. Shawqi, M. A.; Nasir, A. M.; Aziz, F.; Kumar, G.; Sallehhudin, W.; Jaafar, J.; Lau, W. J.; Yusof, N.; Salleh, W. N. W.; Ismail, A. F., CO2/N2 selectivity enhancement of PEBAX MH 1657/Aminated partially reduced graphene oxide mixed matrix composite membrane. *Separation and Purification Technology* **2019,** *223*, 142-153.

75. Wang, D.; Yao, D.; Wang, Y.; Wang, F.; Xin, Y.; Song, S.; Zhang, Z.; Su, F.; Zheng, Y., Carbon nanotubes and graphene oxide-based solvent-free hybrid nanofluids functionalized mixed-matrix membranes for efficient CO2/N2 separation. *Separation and Purification Technology* **2019,** *221*, 421-432.

76. Huang, G.; Isfahani, A. P.; Muchtar, A.; Sakurai, K.; Shrestha, B. B.; Qin, D.; Yamaguchi, D.; Sivaniah, E.; Ghalei, B., Pebax/ionic liquid modified graphene oxide mixed matrix membranes for enhanced CO2 capture. *Journal of Membrane Science* **2018,** *565*, 370-379.

77. Yang, K.; Dai, Y.; Ruan, X.; Zheng, W.; Yang, X.; Ding, R.; He, G., Stretched ZIF-8@GO flake-like fillers via pre-Zn(II)-doping strategy to enhance CO2 permeation in mixed matrix membranes. *Journal of Membrane Science* **2020,** *601*, 117934.

78. Dong, L.; Chen, M.; Li, J.; Shi, D.; Dong, W.; Li, X.; Bai, Y., Metal-organic framework-graphene oxide composites: A facile method to highly improve the CO2 separation performance of mixed matrix membranes. *Journal of Membrane Science* **2016,** *520*, 801-811.

79. Huang, T.-C.; Liu, Y.-C.; Lin, G.-S.; Lin, C.-H.; Liu, W.-R.; Tung, K.-L., Fabrication of pebax-1657-based mixed-matrix membranes incorporating N-doped few-layer graphene for carbon dioxide capture enhancement. *Journal of Membrane Science* **2020,** *602*, 117946.

80. Zhang, J.; Xin, Q.; Li, X.; Yun, M.; Xu, R.; Wang, S.; Li, Y.; Lin, L.; Ding, X.; Ye, H.; Zhang, Y., Mixed matrix membranes comprising aminosilane-functionalized graphene oxide for enhanced CO2 separation. *Journal of Membrane Science* **2019,** *570-571*, 343-354.

81. Zhu, W.; Qin, Y.; Wang, Z.; Zhang, J.; Guo, R.; Li, X., Incorporating the magnetic alignment of GO composites into Pebax matrix for gas separation. *Journal of Energy Chemistry* **2019,** *31*, 1-10.

82. Sutrisna, P. D.; Hou, J.; Zulkifli, M. Y.; Li, H.; Zhang, Y.; Liang, W.; D'Alessandro, Deanna M.; Chen, V., Surface functionalized UiO-66/Pebax-based ultrathin composite hollow fiber gas separation membranes. *Journal of Materials Chemistry A* **2018,** *6* (3), 918-931.

83. Meshkat, S.; Kaliaguine, S.; Rodrigue, D., Mixed matrix membranes based on amine and non-amine MIL-53(Al) in Pebax® MH-1657 for CO2 separation. *Separation and Purification Technology* **2018,** *200*, 177-190.

84. Nafisi, V.; Hägg, M.-B., Development of dual layer of ZIF-8/PEBAX-2533 mixed matrix membrane for CO2 capture. *Journal of Membrane Science* **2014,** *459*, 244-255.

85. Zhao, D.; Ren, J.; Li, H.; Li, X.; Deng, M., Gas separation properties of poly(amide-6-b-ethylene oxide)/amino modified multi-walled carbon nanotubes mixed matrix membranes. *Journal of Membrane Science* **2014,** *467*, 41-47.

86. Zhang, H.; Guo, R.; Hou, J.; Wei, Z.; Li, X., Mixed-Matrix Membranes Containing Carbon Nanotubes Composite with Hydrogel for Efficient CO2 Separation. *ACS Applied Materials & Interfaces* **2016,** *8* (42), 29044-29051.

87. Amir Al, A.; Sultan, A. S.; Zaidi, S. M. J., Sulfonated Poly(Ether Ether Ketone) (SPEEK): A Promising Membrane Material for Polymer Electrolyte Fuel Cell. In *Ion Exchange Technology I: Theory and Materials*, Dr, I.; Luqman, M., Eds. Springer Netherlands: Dordrecht, **2012,** 437-451.

88. Xin, Q.; Ma, F.; Zhang, L.; Wang, S.; Li, Y.; Ye, H.; Ding, X.; Lin, L.; Zhang, Y.; Cao, X., Interface engineering of mixed matrix membrane via CO2-philic polymer brush functionalized graphene oxide nanosheets for efficient gas separation. *Journal of Membrane Science* **2019,** *586*, 23-33.

89. Xin, Q.; Li, Z.; Li, C.; Wang, S.; Jiang, Z.; Wu, H.; Zhang, Y.; Yang, J.; Cao, X., Enhancing the CO2 separation performance of composite membranes by the incorporation of amino acid-functionalized graphene oxide. *Journal of Materials Chemistry A* **2015,** *3* (12), 6629-6641.

90. Xin, Q.; Ouyang, J.; Liu, T.; Li, Z.; Li, Z.; Liu, Y.; Wang, S.; Wu, H.; Jiang, Z.; Cao, X., Enhanced Interfacial Interaction and CO2 Separation Performance of Mixed Matrix Membrane by Incorporating Polyethylenimine-Decorated Metal–Organic Frameworks. *ACS Applied Materials & Interfaces* **2015,** *7* (2), 1065-1077.

91. Xin, Q.; Liu, T.; Li, Z.; Wang, S.; Li, Y.; Li, Z.; Ouyang, J.; Jiang, Z.; Wu, H., Mixed matrix membranes composed of sulfonated poly(ether ether ketone) and a sulfonated metal–organic framework for gas separation. *Journal of Membrane Science* **2015,** *488*, 67-78.

92. Xin, Q.; Zhang, Y.; Shi, Y.; Ye, H.; Lin, L.; Ding, X.; Zhang, Y.; Wu, H.; Jiang, Z., Tuning the performance of CO2 separation membranes by incorporating multifunctional modified silica microspheres into polymer matrix. *Journal of Membrane Science* **2016,** *514*, 73-85.

93. Rose, J. B., Preparation and properties of poly(arylene ether sulphones). *Polymer* **1974,** *15* (7), 456-465.

94. Shen, Y.; Wang, H.; Liu, J.; Zhang, Y., Enhanced Performance of a Novel Polyvinyl Amine/Chitosan/Graphene Oxide Mixed Matrix Membrane for CO2 Capture. *ACS Sustainable Chemistry & Engineering* **2015,** *3* (8), 1819-1829.

95. Wang, Y.; Li, L.; Zhang, X.; Li, J.; Liu, C.; Li, N.; Xie, Z., Polyvinylamine/graphene oxide/PANI@CNTs mixed matrix composite membranes with enhanced CO2/N2 separation performance. *Journal of Membrane Science* **2019,** *589*, 117246.

96. Dong, G.; Zhang, Y.; Hou, J.; Shen, J.; Chen, V., Graphene Oxide Nanosheets Based Novel Facilitated Transport Membranes for Efficient CO2 Capture. *Industrial & Engineering Chemistry Research* **2016,** *55* (18), 5403-5414.

97. Anastasiou, S.; Bhoria, N.; Pokhrel, J.; Kumar Reddy, K. S.; Srinivasakannan, C.; Wang, K.; Karanikolos, G. N., Metal-organic framework/graphene oxide composite fillers in mixed-matrix membranes for CO2 separation. *Materials Chemistry and Physics* **2018,** *212*, 513-522.

98. Sarfraz, M.; Ba-Shammakh, M., Synergistic effect of adding graphene oxide and ZIF-301 to polysulfone to develop high performance mixed matrix membranes for selective carbon dioxide separation from post combustion flue gas. *Journal of Membrane Science* **2016,** *514*, 35-43.

99. Chang, Y.-W.; Chang, B. K., Influence of casting solvents on sedimentation and performance in metal–organic framework mixed-matrix membranes. *Journal of the Taiwan Institute of Chemical Engineers* **2018,** *89*, 224-233.

100. Sarfraz, M.; Ba-Shammakh, M., A novel zeolitic imidazolate framework based mixed-matrix membrane for efficient CO2 separation under wet conditions. *Journal of the Taiwan Institute of Chemical Engineers* **2016,** *65*, 427-436.

101. Chen, B.; Wan, C.; Kang, X.; Chen, M.; Zhang, C.; Bai, Y.; Dong, L., Enhanced CO2 separation of mixed matrix membranes with ZIF-8@GO composites as fillers: Effect of reaction time of ZIF-8@GO. *Separation and Purification Technology* **2019,** *223*, 113-122.

102. Yang, K.; Dai, Y.; Zheng, W.; Ruan, X.; Li, H.; He, G., ZIFs-modified GO plates for enhanced CO2 separation performance of ethyl cellulose based mixed matrix membranesf. *Separation and Purification Technology* **2019,** *214*, 87-94.

103. Farmer, S. Fischer Esterification. https://chem.libretexts.org/Bookshelves/Organic_Chemistry/Supplemental_Modules_(Organic_Chemistry)/Carboxylic_Acids/Reactivity_of_Carboxylic_Acids/Fischer_Esterification (accessed 18.06.20).

104. Carey, F., Organic Chemistry. *New York: McGraw-Hill.* **2006,** *6th edition*, 866-888.

105. Economopoulos, S.; Pagona, G.; Yudasaka, M.; Iijima, S.; Tagmatarchis, N., Solvent-Free Microwave-Assisted Bingel Reaction in Carbon Nanohorns. *Journal of Materials Chemistry - Journal of Material Chemistry* **2009,** *19*.

106. Lucasen, S. M. Synthesis and evaluation of nanohybrid materials for the solid-phase extraction of trace organic pollutants from water samples. Norwegian University of Science and Technology, Trondheim, **2020**.

Appendix

^{1}H-NMR Spectrums

In this appendix, ^{1}H-NMR spectrums and assigned shifts will be presented of A) 2-(2-(2-ethoxy ethoxy)ethoxy)ethyl 4-(pyren-2-yl)butanoate and B) of 2-(2-(2-ethoxy ethoxy)ethoxy)ethyl ethyl malonate. The pyrenyl-butanoate was diluted with impurities and starting material, but there were traces of product. The malonate, on the other hand, was relatively pure.

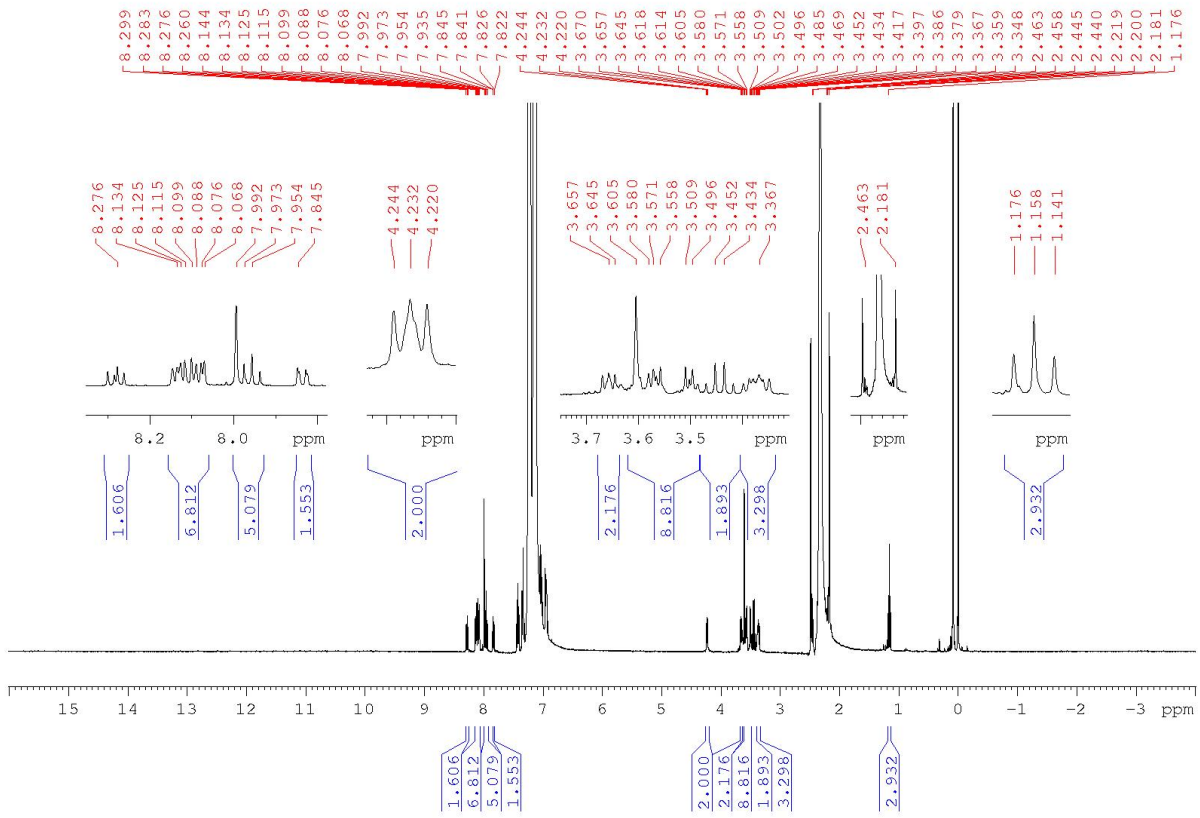

Spectrum A: ^{1}H-NMR of 2-(2-(2-ethoxy ethoxy)ethoxy)ethyl 4-(pyren-2-yl)butanoate.

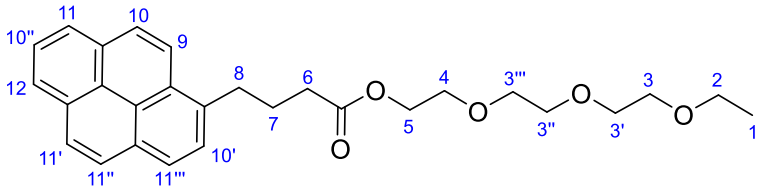

Figure A.1: 2-(2-(2-Ethoxy ethoxy)ethoxy)ethyl 4-(pyren-2-yl)butanoate crude with numerated positions.

Table A.1: Proton shifts, multiplicity, integrals, and coupling constants for the 2-(2-(2-ethoxy ethoxy)ethoxy)ethyl 4-(pyren-2-yl)butanoate crude, assigned to positions shown in Fig. A.1.

Position in Fig. A.1	δ_H [ppm]	Multiplicity	Integral [#H]	*J* [Hz]
1	1.15	t	3	7.1
2	3.44	q	2	7.0
3/3’/3’’/3’’’	3.61-3.48	m	8	-
4	3.65	t	2	5.1
5	4.23	t	2	4.8
6	2.46-2.44	m	- (2*)	-
7	2.21-2.18	m	- (2*)	-
8	3.38-3.34	m	3.2 (2*)	
9	7.84-7.82	m	1.6 (1*)	-
10/10’/10’’	7.99-7.93	m	6.8 (4*)	-
11/11’/11’’/11’’’	8.14-8.06	m	5.1 (3*)	-
12	8.29-8.26	m	1.6 (1*)	-

* #H supposed to be in the pure product

Due to the time constrained not allowing to complete the work up of the crude, full characterization, involving ^{13}C-NMR, MS etc., was not performed. ^{1}H-NMR integrals signified that there were traces from the acid starting material remaining in the crude, but it looked like the alcohol was fully utilized. Position 6 and 7 were peaks overlapped by other impurities and were difficult to analyse. However, the triplet at 4.23 ppm (position 5) indicated presence of product, leaving this approach to be transmitted to future work.

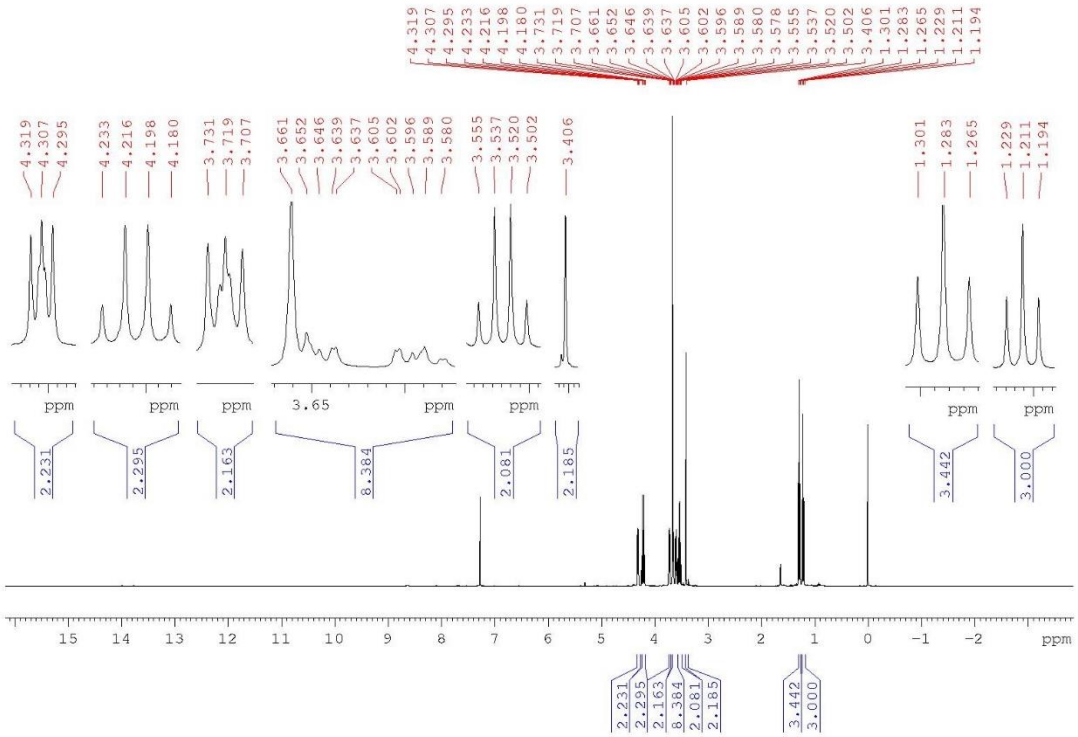

Spectrum B: ^{1}H-NMR of 2-(2-(2-ethoxy ethoxy)ethoxy)ethyl ethyl malonate.

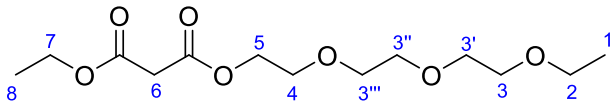

Figure B.1: 2-(2-(2-ethoxy ethoxy)ethoxy)ethyl ethyl malonate with numerated positions.

Table B.1: Proton shifts, multiplicity, integrals, and coupling constants for the 2-(2-(2-ethoxy ethoxy)ethoxy)ethyl ethyl malonate, assigned to positions shown in Fig. A.2.

Position in **Fig. B.1**	δ_H [ppm]	Multiplicity	Integral [#H]	*J* [Hz]
1	1.21	t	3	7.1
2	3.52	q	2	7.0
3/3'/3''/3'''	3.66-3.57	m	8	-
4	3.71	t	2	5.0
5	4.30	t	2	4.8
6	3.40	s	2	-
7	4.20	q	2	7.0
8	1.28	t	3	7.2

Since this was a synthesis according to the lab procedure, full characterization was not performed for this product either. However, through ^{1}H-NMR the product was characterized relatively straightforward, due to the multiplicity discerning and separating the hydrocarbons nicely. This approach would therefore also be transmitted to future work.

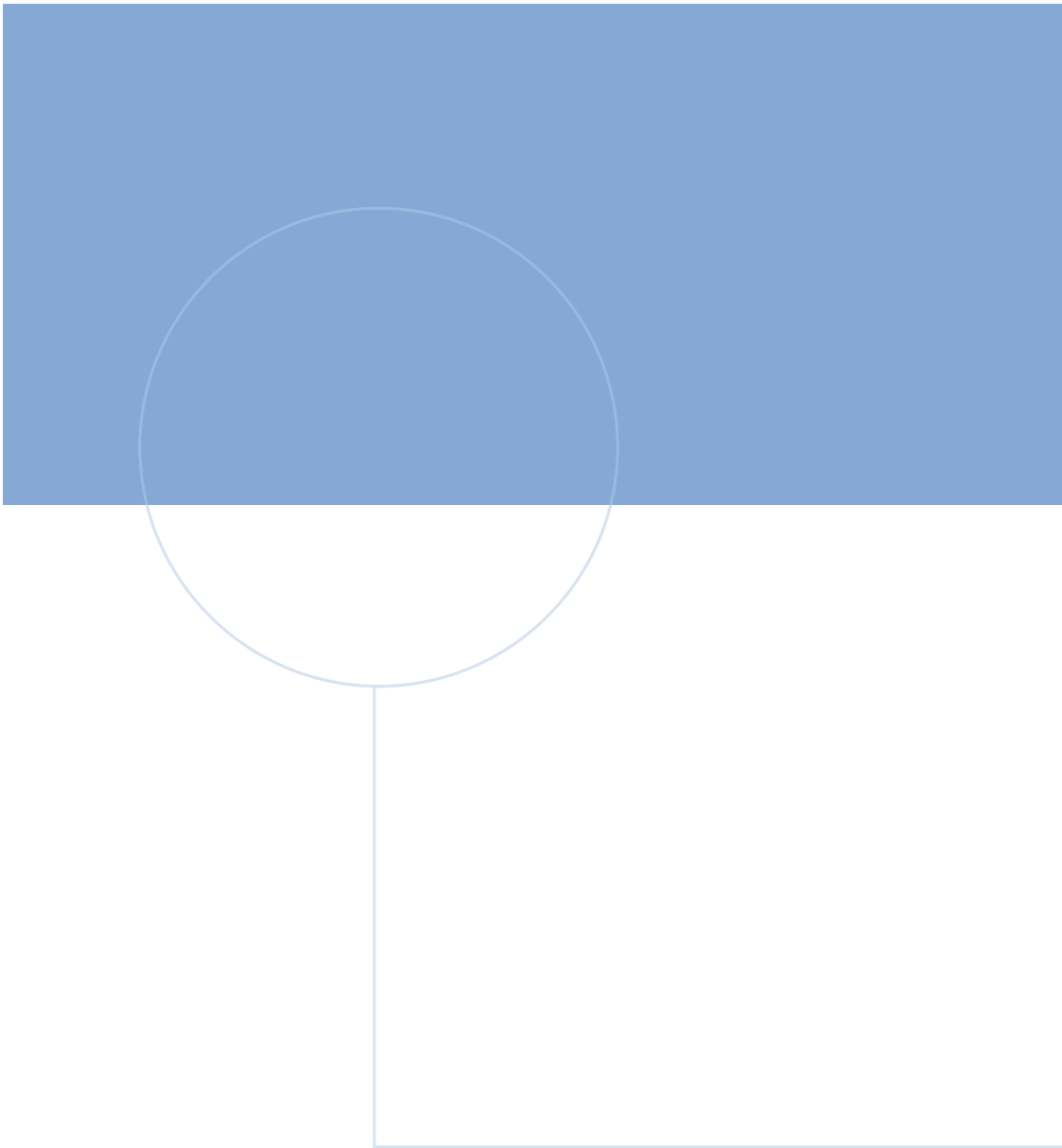

NTNU

Norwegian University of
Science and Technology